

# A Two-Surface Problem of the Electron Flow in a Semiconductor on the Basis of Kinetic Theory

Satoshi Taguchi · Ansgar Jüngel

Received: 27 April 2007 / Accepted: 4 September 2007 / Published online: 3 October 2007  
© Springer Science+Business Media, LLC 2007

**Abstract** A steady flow of electrons in a semiconductor between two parallel plane Ohmic contacts is studied on the basis of the semiconductor Boltzmann equation, assuming a relaxation-time collision term, and the Poisson equation for the electrostatic potential. A systematic asymptotic analysis of the Boltzmann–Poisson system for small Knudsen numbers (scaled mean free paths) is carried out in the case where the Debye length is of the same order as the distance between the contacts and where the applied potential is of the same order as the thermal potential. A system of drift-diffusion-type equations and their boundary conditions is obtained up to second order in the Knudsen number. A numerical comparison is made between the obtained system and the original Boltzmann–Poisson system.

**Keywords** Semiconductor Boltzmann equation · Hilbert expansion · Drift-diffusion equations · Second-order boundary conditions

## 1 Introduction

Precise simulations of classical carrier transport in modern semiconductor devices are usually performed using the semiconductor Boltzmann equation. However, this equation requires large computing times and is therefore inconvenient for the solution of real problems in semiconductor production mode. Therefore, simpler models have been derived which focus only on the first few moments of the velocity distribution function. For instance, the drift-diffusion model [1] comprises the first two moments, whereas the hydrodynamic model [2] contains three moments and the energy-transport model [3] four moments (see [4, 5] for a mathematical derivation of the latter model, [6, 7] for the mathematical theory, and [8] for the numerical discretization). Also higher-order models have been investigated [9, 10].

---

S. Taguchi

Organization of Advanced Science and Technology, Kobe University, Kobe 657-8501, Japan  
e-mail: taguchi@mech.kobe-u.ac.jp

A. Jüngel (✉)

Institute for Analysis and Scientific Computing, Vienna University of Technology,  
Wiedner Hauptstr. 8-10, 1040 Wien, Austria  
e-mail: juengel@anum.tuwien.ac.at

The drift-diffusion equations and their variants are the most utilized model in industrial semiconductor simulations since there exist very efficient numerical schemes and since it gives reasonable results even in far-from-equilibrium situations for moderate device lengths. Moreover, higher-order transport models have not been widely accepted as a viable substitute since they are numerically more complex and they contain several transport parameters, which are not always easy to determine or to fit to Monte-Carlo data.

Besides of the choice of the model equations, the modeling of accurate boundary conditions is another problem which is rarely addressed in the existing literature. Yamnahakki [11] derived for the drift-diffusion model improved boundary conditions of Robin type, by considering a correction due to the non-vanishing mean free path. More specifically, he derived a higher-order boundary condition up to *first order* in the (small) Knudsen number (i.e., the mean free path scaled by the characteristic length). However, no comparison with the current density resulting from the solution of the Boltzmann equation has been made. Improved inflow-type boundary conditions for the kinetic models have been suggested in [12, 13], but no macroscopic boundary conditions have been derived.

The problem considered by Yamnahakki in [11] is a problem of a one-dimensional electron flow in a slab (two-surface problem of electrons) on the basis of a semiconductor Boltzmann equation. This is a classical problem which has been investigated in the physical [14–19] and mathematical [11] literature. For example, in [14, 15, 18, 19], the feature of the velocity distribution function peculiar to the ballistic transport has been clarified by means of a direct numerical simulation of Boltzmann–Poisson systems in  $n^+nn^+$  structures. In these analyses, however, the effect of the boundary has been deliberately removed by making use of a long  $n^+$  region. Therefore, the problem including the effect of the boundary has not been fully solved. On the other hand, [11] provides a complete mathematical theory of the problem including the kinetic boundary conditions. However, the detailed flow pattern is not given there, since the purpose of the work is to clarify the mathematical structure of the problem. Further, in order to obtain precise mathematical results, the electric field is assumed to be given so that only the linear Boltzmann equation has been considered (i.e., no Poisson equation).

In this paper, we investigate the two-surface problem of the electron flow by means of a systematic asymptotic analysis for the small Knudsen numbers. We derive, for the first time, drift-diffusion-type equations together with their boundary conditions up to *second order* in the Knudsen number and compare the results with the direct solution of the Boltzmann–Poisson system.

Our approach is essentially the same as that used in the work of Yamnahakki to derive the Robin-type boundary condition mentioned above. In fact, we employ the classical Hilbert expansion method, which has been applied to the semiconductor Boltzmann equation by many authors. We refer to [20, 21] as pioneering papers on this subject, and to [22] for the first construction of the boundary-layer corrections to the transport equation. It should also be mentioned that the same method is used to derive higher-order boundary condition for the SHE model and the energy-transport model [23]. In a more physical context, the Hilbert expansion has been used in connection with the asymptotic analysis of the Boltzmann equation for small Knudsen numbers employed in kinetic gas theory, developed by Sone and co-workers [24–32]. In these works, no external force has been imposed. Recently, the same asymptotic analysis has been used to investigate a rarefied gas flow between two parallel plates driven by a *uniform* external force parallel to the plate [33] on the basis of the Bhatnagar–Gross–Krook (BGK) model [34–36] of the Boltzmann equation. In this paper, our asymptotic analysis follows those in [24–32], since it provides a systematic way to investigate the effect of the non-vanishing mean free path on the flow property.

It should be noted that, in the present study, we make rather strong assumptions in order to simplify the boundary-value problem and to make numerical comparisons more feasible. First, we assume that the collision operator is given by a relaxation model similar to the BGK model. A more general collision term can be employed (see [11]), but a specific choice has to be made in order to compute the Milne problem arising in the asymptotic analysis. In addition, more realistic collision operators make the direct solution of the Boltzmann equation, which is needed for comparison, much more complicate. Second, we consider the time-independent problem. However, the extension to the time-dependent case can be done in a straightforward way. Third, for the asymptotic analysis, we assume that the Debye length is of the same order as the distance between the contacts (or the device length) and that the applied voltage is of the same order as the thermal potential. The latter condition is not restricting in practice since the drift-diffusion model gives reasonable results even for larger applied voltages. However, the former assumption imposes a condition on the magnitude of the doping profile, which should not be too large. In fact, our results are valid in or close to the channel region of an  $n^+nn^+$  diode (where the doping concentration is indeed small) and could in particular help for the derivation of interface conditions for hybrid models in which the highly doped regions and the channel region are described by different models. Finally, we point out again that the Poisson equation has been discarded in the analysis of Yamnahakki, which results in the absence of the Debye length in the parameter set.

The paper is organized as follows. After formulating the problem (Sect. 2), we carry out a systematic asymptotic analysis of the Boltzmann–Poisson system for small Knudsen numbers (Sect. 3). We derive a system of fluid-dynamic equations and their boundary conditions on the contacts up to second order of the Knudsen number. In Sect. 4, we perform a numerical comparison between the solutions of the derived fluid-dynamic systems and the direct solution of the original Boltzmann–Poisson system on a simple  $n^+nn^+$  diode which can be considered as a model for the channel region of a MOS transistor.

## 2 Formulation of the Problem

### 2.1 Problem and Basic Assumptions

We consider a semiconductor between two plane Ohmic contacts located at  $X_1 = 0$  (contact  $A$ ) and  $X_1 = L$  (contact  $B$ ), where  $X_i$  is a rectangular space coordinate system. Let  $T_0$  be the temperature of the semiconductor lattice as well as that of the contacts, and let  $\phi_A$  and  $\phi_B$  be the electric potentials applied at the contacts  $A$  and  $B$ , respectively. We investigate the steady behavior of the electron flow in the  $X_1$  direction induced in the semiconductor under the following assumptions: (i) The behavior of the electrons is described by the semiconductor Boltzmann equation in the parabolic band approximation, employing a relaxation-time collision operator. The electrostatic potential is self-consistently computed from the Poisson equation. (ii) The velocity distribution of the electrons leaving the contact is described by the corresponding part of the Maxwellian distribution with temperature  $T_0$  and zero flow velocity, fulfilling the charge-neutral condition. In the following, we restrict ourselves to the following physical situation: (i) The Knudsen number is small. (ii) The Debye length is of the same order as the distance between the contacts. (iii) The potential difference between the contacts is of the same order as the thermal potential. Thanks to these assumptions, a diffusion approximation of the Boltzmann equation can be performed. This approximation can be made mathematically rigorous; see, e.g., [20, 21].

### 2.2 Basic Equations

Let  $v_i$  be the electron velocity,  $f(X_1, v_i)$  the velocity distribution function of the electrons,  $(E(X_1), 0, 0)$  the electric field,  $m^*$  the effective electron mass,  $q$  the elementary charge, and  $k$  the Boltzmann constant. Then, under the parabolic band approximation, the Boltzmann equation with a relaxation-time collision operator is written for the present stationary one-dimensional problem as

$$v_1 \frac{\partial f}{\partial X_1} - \frac{q}{m^*} E \frac{\partial f}{\partial v_1} = \frac{1}{\tau} (\rho M - f), \tag{1}$$

where

$$M = \frac{1}{(2\pi kT_0/m^*)^{3/2}} \exp\left(-\frac{v_i^2}{2kT_0/m^*}\right) \tag{2}$$

is the Maxwellian,  $\rho = \int f d^3v$  the electron number density,  $\tau(X_1)$  is the electron relaxation time, and  $d^3v = dv_1 dv_2 dv_3$ . The summation convention is employed. Here and in the following, the integral with respect to  $v_i$  is carried out over the whole space. The electric field  $E$  is calculated from the electrostatic potential  $\phi(X_1)$  by  $E = -d\phi/dX_1$ , where  $\phi(X_1)$  solves the Poisson equation

$$\epsilon_s \frac{d^2\phi}{dX_1^2} = q(\rho - C). \tag{3}$$

Here,  $\epsilon_s$  is the permittivity of the semiconductor and  $C(X_1)$  is the doping profile which is assumed to be smooth.

Under the charge neutral condition, the boundary condition on the contact  $A$  ( $X_1 = 0$ ) is given by

$$f = C(0)M \quad \text{for } v_1 > 0, \quad \phi = \phi_A, \tag{4}$$

whereas the boundary condition on the contact  $B$  ( $X_1 = L$ ) reads as

$$f = C(L)M \quad \text{for } v_1 < 0, \quad \phi = \phi_B. \tag{5}$$

Finally, let us define some macroscopic quantities. Let  $(J(X_1), 0, 0)$  denote the electron current density,  $(u(X_1), 0, 0)$  the electron mean velocity, and  $T(X_1)$  the electron temperature. They are defined as

$$J = -q\rho u = -q \int v_1 f d^3v, \quad T = \frac{m^*}{3k\rho} \int (v_i - u\delta_{i1})^2 f d^3v.$$

### 2.3 Dimensionless Variables

Let  $\rho_0$  and  $\tau_0$  be, respectively, characteristic values of the electron number density and of the relaxation time, and let  $U_T = kT_0/q$  be the thermal potential related to the lattice tem-

perature  $T_0$ . We introduce the following dimensionless quantities:

$$\begin{aligned}
 x_i &= \frac{X_i}{L}, & \zeta_i &= \frac{v_i}{(2kT_0/m^*)^{1/2}}, & \hat{f} &= \frac{(2kT_0/m^*)^{3/2}}{\rho_0} f, \\
 \hat{\tau} &= \frac{\tau}{\tau_0}, & \hat{\phi} &= \frac{\phi}{U_T}, & \hat{E} &= \frac{E}{U_T/L}, & \hat{C} &= \frac{C}{\rho_0}, & \hat{\rho} &= \frac{\rho}{\rho_0}, \\
 \hat{J} &= -\frac{J}{q\rho_0(2kT_0/m^*)^{1/2}}, & \hat{u} &= \frac{u}{(2kT_0/m^*)^{1/2}}, & \hat{T} &= \frac{T}{T_0}.
 \end{aligned}$$

Using these dimensionless quantities, the Boltzmann–Poisson system (1–3) becomes

$$\zeta_1 \frac{\partial \hat{f}}{\partial x_1} - \frac{1}{2} \hat{E} \frac{\partial \hat{f}}{\partial \zeta_1} = \frac{2}{\sqrt{\pi}} \frac{1}{\text{Kn}} \frac{1}{\hat{\tau}} (\hat{\rho} \mathcal{M} - \hat{f}), \quad \mathcal{M} = \frac{1}{\pi^{3/2}} \exp(-\zeta_i^2), \tag{6}$$

$$\hat{\rho} = \int \hat{f} d^3 \zeta, \tag{7}$$

$$\lambda^2 \frac{d^2 \hat{\phi}}{dx_1^2} = \hat{\rho} - \hat{C}, \tag{8}$$

$$\hat{E} = -\frac{d\hat{\phi}}{dx_1}, \tag{9}$$

$$\text{Kn} = \frac{l_0}{L} = \frac{2}{\sqrt{\pi}} \frac{(2kT_0/m^*)^{1/2} \tau_0}{L}, \quad \lambda = \frac{\lambda_0}{L} = \sqrt{\frac{\epsilon_s U_T}{q\rho_0 L^2}}, \tag{10}$$

where  $d^3 \zeta = d\zeta_1 d\zeta_2 d\zeta_3$ . Again, here and in the following, the domain of integration with respect to  $\zeta_i$  is the whole space. The dimensionless parameter Kn, which is defined by the ratio of the mean free path of an electron  $l_0 = (2/\sqrt{\pi})(2kT_0/m^*)^{1/2} \tau_0$  to the distance  $L$  between the contacts, is called the Knudsen number (or scaled mean free path), and represents the frequency of collisions of an electron with other particles (phonons, impurities etc.). The dimensionless parameter  $\lambda$ , defined by the ratio of the Debye length  $\lambda_0 = (\epsilon_s U_T / q\rho_0)^{1/2}$  of the semiconductor to the distance  $L$  between the contacts, is called the scaled Debye length. The dimensionless form of the boundary conditions is written as

$$\hat{f} = \hat{C}(0) \mathcal{M} \quad \text{for } \zeta_1 > 0, \quad \hat{\phi} = \hat{\phi}_A \text{ at } x_1 = 0, \tag{11}$$

$$\hat{f} = \hat{C}(1) \mathcal{M} \quad \text{for } \zeta_1 < 0, \quad \hat{\phi} = \hat{\phi}_B \text{ at } x_1 = 1, \tag{12}$$

where  $(\hat{\phi}_A, \hat{\phi}_B) = (\phi_A / U_T, \phi_B / U_T)$ . Finally, the dimensionless macroscopic quantities are expressed in terms of the dimensionless velocity distribution function as follows:

$$\hat{J} = \hat{\rho} \hat{u} = \int \zeta_1 \hat{f} d^3 \zeta, \tag{13}$$

$$\hat{T} = \frac{2}{3\hat{\rho}} \int (\zeta_i - \hat{u} \delta_{i1})^2 \hat{f} d^3 \zeta. \tag{14}$$

The functions  $\hat{\tau}(x_1)$  and  $\hat{C}(x_1)$  are specified according to the specific semiconductor device. Once they are given, the present boundary-value problem is characterized by the parameters Kn,  $\lambda$ , and  $\hat{\phi}_A - \hat{\phi}_B$ . In the present study, we investigate the behavior of the

electron flow for small Knudsen numbers  $\text{Kn} \ll 1$  when both the scaled Debye length  $\lambda$  and the (dimensionless) potential difference  $|\hat{\phi}_B - \hat{\phi}_A|$  are of the order one. Incidentally, the integration of (6) with respect to  $\zeta_i$  over the whole space leads to  $d\hat{J}/dx_1 = 0$ , and therefore, we have  $\hat{J} = \text{const}$  for all  $0 \leq x_1 \leq 1$ .

### 3 Asymptotic Analysis and Fluid-Dynamic Equations

In this section, we carry out an asymptotic analysis of the Boltzmann–Poisson system described in the previous section when the scaled Debye length  $\lambda$  and the potential difference  $|\hat{\phi}_B - \hat{\phi}_A|$  are of the order of unity. In the course of the analysis, we derive some drift-diffusion-type equations, coupled with the Poisson equation, as well as their boundary conditions. In the following, we use  $\epsilon = (\sqrt{\pi}/2)\text{Kn}$  as a small parameter rather than the Knudsen number  $\text{Kn}$  itself.

#### 3.1 Hilbert Solution

First, putting aside the boundary conditions, we look for a solution  $(\hat{f}_H, \hat{\phi}_H)$  to (6–9) which varies moderately over the distance between the contacts, i.e.,  $\partial \hat{f}_H / \partial x_1 = O(\hat{f}_H)$  and  $d\hat{\phi}_H / dx_1 = O(\hat{\phi}_H)$ . Such a solution is called the *Hilbert solution* and is denoted by the subscript  $H$ . We assume that  $\hat{f}_H$  and  $\hat{\phi}_H$  can be expressed in powers of  $\epsilon$ , i.e.,

$$\hat{f}_H = \hat{f}_{H0} + \hat{f}_{H1}\epsilon + \hat{f}_{H2}\epsilon^2 + \dots, \tag{15}$$

$$\hat{\phi}_H = \hat{\phi}_{H0} + \hat{\phi}_{H1}\epsilon + \hat{\phi}_{H2}\epsilon^2 + \dots. \tag{16}$$

Correspondingly, the macroscopic variables  $h$  (where  $h = \hat{\rho}_H, \hat{J}_H, \hat{u}_H$ , or  $\hat{T}_H$ ) as well as the electric field  $\hat{E}_H$  are expanded in  $\epsilon$  as

$$h_H = h_{H0} + h_{H1}\epsilon + h_{H2}\epsilon^2 + \dots, \tag{17}$$

$$\hat{E}_H = \hat{E}_{H0} + \hat{E}_{H1}\epsilon + \hat{E}_{H2}\epsilon^2 + \dots. \tag{18}$$

The relation between  $\hat{f}_{Hm}$  and  $h_m$  is obtained by substituting (15) and (17) into (7, 13), and (14) with  $h = h_H$  and  $\hat{f} = \hat{f}_H$  and equating the coefficients with the same power of  $\epsilon$ . For  $h = \hat{\rho}_H$  or  $\hat{J}_H$ , we find

$$\hat{\rho}_{Hm} = \int \hat{f}_{Hm} d^3\zeta, \tag{19}$$

$$\hat{J}_{Hm} = \int \zeta_1 \hat{f}_{Hm} d^3\zeta \quad (m = 0, 1, \dots). \tag{20}$$

We omit the results for  $\hat{u}_H$  and  $\hat{T}_H$  for conciseness. Similarly, the relation between  $\hat{\phi}_{Hm}$  and  $\hat{E}_{Hm}$  is obtained by substituting (16) and (18) into (9) with  $\hat{E} = \hat{E}_H$  and  $\hat{\phi} = \hat{\phi}_H$  and equating the coefficients with the same power of  $\epsilon$ . [Here, we keep in mind the property  $d\hat{\phi}_H / dx_1 = O(\hat{\phi}_H)$ .] Thus, we have

$$\hat{E}_{Hm} = -\frac{d\hat{\phi}_{Hm}}{dx_1} \quad (m = 0, 1, \dots). \tag{21}$$

Since our collision term conserves the number of particles, it holds  $\int (\hat{\rho}_H \mathcal{M} - \hat{f}_H) d^3 \zeta = 0$ , and hence,

$$\int (\hat{\rho}_{Hm} \mathcal{M} - \hat{f}_{Hm}) d^3 \zeta = 0 \quad (m = 0, 1, \dots). \tag{22}$$

Substituting (15, 17) (with  $h = \hat{\rho}$ ), and (18) into (6) and taking into account the property  $\partial \hat{f}_H / \partial x_1 = O(\hat{f}_H)$  gives the following expressions for  $\hat{f}_{Hm}$ :

$$\hat{f}_{H0} = \hat{\rho}_{H0} \mathcal{M}, \tag{23}$$

$$\hat{f}_{Hm} = \hat{\rho}_{Hm} \mathcal{M} - \hat{\tau} \left( \zeta_1 \frac{\partial \hat{f}_{Hm-1}}{\partial x_1} - \frac{1}{2} \sum_{n=0}^{m-1} \hat{E}_{Hn} \frac{\partial \hat{f}_{Hm-n-1}}{\partial \zeta_1} \right) \quad (m \geq 1). \tag{24}$$

Equation (22) provides the compatibility conditions for (24), i.e.,

$$0 = \int \left( \zeta_1 \frac{\partial \hat{f}_{Hm-1}}{\partial x_1} - \sum_{n=0}^{m-1} \frac{\hat{E}_{Hn}}{2} \frac{\partial \hat{f}_{Hm-n-1}}{\partial \zeta_1} \right) d^3 \zeta = \frac{d}{dx_1} \int \zeta_1 \hat{f}_{Hm-1} d^3 \zeta \quad (m \geq 1). \tag{25}$$

When we use in (25) the explicit expressions for  $\hat{f}_{Hn}$  ( $n = 0, 1, \dots$ ) in terms of  $\hat{\rho}_{Hs}$  ( $s \leq n$ ) and  $\hat{E}_{Hs}$  ( $s \leq n - 1$ ), which are obtained successively from (23) and (24), we derive ordinary differential equations for  $\hat{\rho}_{Hn}$  and  $\hat{E}_{Hn}$ , called here *fluid-dynamic equations*.

Furthermore, when we substitute (16) and (17) (with  $h = \hat{\rho}$ ) into (8) with  $\hat{\phi} = \hat{\phi}_H$  and  $\hat{\rho} = \hat{\rho}_H$  and take into account the property  $d\hat{\phi}_H/dx_1 = O(\hat{\phi}_H)$  as well as  $\lambda = O(1)$ , we obtain the following sequence of equations:

$$\lambda^2 \frac{d^2 \hat{\phi}_{H0}}{dx_1^2} = \hat{\rho}_{H0} - \hat{C}, \quad \lambda^2 \frac{d^2 \hat{\phi}_{Hm}}{dx_1^2} = \hat{\rho}_{Hm} \quad (m \geq 1).$$

These equations are coupled with the fluid-dynamic equations through (21).

In this paragraph, we summarize the systems of fluid-dynamic equations. First, we note that (23) and (20) imply that  $\hat{J}_{H0} = 0$ . Therefore, (25) for  $m = 1$  [with (20)] does not give any condition for the macroscopic quantities. Equation (25) for  $m \geq 2$ , together with the explicit expression for  $\hat{J}_{Hm}$  ( $m \geq 1$ ), gives the following fluid-dynamic equations: for  $m = 0$ ,

$$\frac{d}{dx_1} \hat{J}_{H1} = 0, \tag{26a}$$

$$\hat{J}_{H1} = -\frac{1}{2} \hat{\tau} \left( \frac{d\hat{\rho}_{H0}}{dx_1} + \hat{\rho}_{H0} \hat{E}_{H0} \right), \tag{26b}$$

$$\hat{E}_{H0} = -\frac{d\hat{\phi}_{H0}}{dx_1}, \quad \lambda^2 \frac{d^2 \hat{\phi}_{H0}}{dx_1^2} = \hat{\rho}_{H0} - \hat{C}, \tag{26c}$$

for  $m = 1$ ,

$$\frac{d}{dx_1} \hat{J}_{H2} = 0, \tag{27a}$$

$$\hat{J}_{H2} = -\frac{1}{2} \hat{\tau} \left( \frac{d\hat{\rho}_{H1}}{dx_1} + \hat{\rho}_{H1} \hat{E}_{H0} + \hat{\rho}_{H0} \hat{E}_{H1} \right), \tag{27b}$$

$$\hat{E}_{H1} = -\frac{d\hat{\phi}_{H1}}{dx_1}, \quad \lambda^2 \frac{d^2 \hat{\phi}_{H1}}{dx_1^2} = \hat{\rho}_{H1}, \tag{27c}$$

and for  $m = 2$ ,

$$\frac{d}{dx_1} \hat{J}_{H3} = 0, \tag{28a}$$

$$\hat{J}_{H3} = -\frac{1}{2} \hat{\tau} \left( \frac{d\hat{\rho}_{H2}}{dx_1} + \hat{\rho}_{H0} \hat{E}_{H2} + \hat{\rho}_{H1} \hat{E}_{H1} + \hat{\rho}_{H2} \hat{E}_{H0} \right) + \hat{\tau} \frac{d}{dx_1} (\hat{\tau} \hat{E}_{H0}) \hat{J}_{H1}, \tag{28b}$$

$$\hat{E}_{H2} = -\frac{d\hat{\phi}_{H2}}{dx_1}, \quad \lambda^2 \frac{d^2 \hat{\phi}_{H2}}{dx_1^2} = \hat{\rho}_{H2}. \tag{28c}$$

Equations (26a–26c) are the well-known drift-diffusion equations for the leading-order quantities  $\hat{\rho}_{H0}$ ,  $\hat{E}_{H0}$ , and  $\hat{\phi}_{H0}$ . Equations (27a–27c) for the variables  $\hat{\rho}_{H1}$ ,  $\hat{E}_{H1}$ , and  $\hat{\phi}_{H1}$  also correspond to a drift-diffusion model, since they can be obtained from a drift-diffusion system (with the mobility given by  $\mu = q\tau/m^*$ ) by means of the expansion corresponding to (15–18). However, the next-order equations (28a–28c) for the variables  $\hat{\rho}_{H2}$ ,  $\hat{E}_{H2}$ , and  $\hat{\phi}_{H2}$  do not constitute a drift-diffusion model due to the last term in (28b).

The presence of the last term in (28b) can be understood in the following way. Suppose that the first order current density (or the particle flux)  $\hat{J}_{H1}$  has been established. Since each electron is accelerated by the electric field and acquires a momentum, the particle flux  $\hat{J}_{H1}$  also introduces a momentum flux. The contribution of these electrons, accelerated by  $\hat{E}_{H0}$  during the period of the order of the relaxation time  $\hat{\tau}$  (or the mean free time), to the momentum flux is counted to be proportional to  $\hat{\tau} \hat{E}_{H0} \hat{J}_{H1}$ . Therefore, if its gradient [cf. the last term of (28b)] is not zero, there is a net accumulation of the momentum at a point under consideration, resulting in a force exerted on the fluid. Consequently, a current flow is induced.

Using the explicit expressions for  $\hat{f}_{Hm}$ , we readily obtain the equations for the mean flow velocity  $\hat{u}_{Hm}$  and the electron temperature  $\hat{T}_{Hm}$ . The results up to  $m = 3$  are given in Appendix 1.

### 3.2 Knudsen Layers and Boundary Conditions for Fluid-Dynamic Equations

In this section we derive the boundary conditions for the fluid-dynamic equations. Suppose that  $\hat{\rho}_{H0}$  and  $\hat{\phi}_{H0}$  take the following values on the boundary:

$$\hat{\rho}_{H0} = \hat{C}(0), \quad \hat{\phi}_{H0} = \hat{\phi}_A \quad \text{at } x_1 = 0, \tag{29}$$

$$\hat{\rho}_{H0} = \hat{C}(1), \quad \hat{\phi}_{H0} = \hat{\phi}_B \quad \text{at } x_1 = 1. \tag{30}$$

With this choice of values, the leading-order velocity distribution function  $\hat{f}_{H0}$  (23) and the leading-order electrostatic potential  $\hat{\phi}_{H0}$  satisfy the boundary conditions (11) and (12). Therefore, (29) and (30) give consistent boundary conditions for the leading-order fluid-dynamic equations (26a–26c). For the higher-order quantities, however, the Hilbert solution does not have enough freedom to satisfy the boundary conditions. Therefore, we need to introduce a so-called Knudsen-layer correction near the boundary.

From now on, we seek the solution in the form

$$\hat{f} = \hat{f}_H + \hat{f}_K, \tag{31}$$

$$\hat{\phi} = \hat{\phi}_H + \hat{\phi}_K, \tag{32}$$

where  $(\hat{f}_K, \hat{\phi}_K)$ , which is called the *Knudsen-layer part*, is the correction to the Hilbert solution  $(\hat{f}_H, \hat{\phi}_H)$  appreciable only in thin layers of thickness of order  $\epsilon$  (or of the mean



free path in the dimensional  $X_1$  variable) adjacent to the boundary. In order to analyze the Knudsen layers near  $x_1 = 0$  and  $x_1 = 1$  simultaneously, it is convenient to introduce the following new variables:

$$\begin{aligned} y = x_1, & \quad \eta = y/\epsilon, & \quad \zeta_y = \zeta_1 & \quad \text{around } x_1 = 0, \\ y = 1 - x_1, & \quad \eta = y/\epsilon, & \quad \zeta_y = -\zeta_1 & \quad \text{around } x_1 = 0. \end{aligned}$$

Here,  $y$ , whose origin is on the boundary, is the coordinate normal to the boundary pointing to the semiconductor,  $\eta$  is the stretched coordinate normal to the boundary, and  $\zeta_y$  is the component of  $\zeta_1$  in the positive  $y$  direction. We assume that the length scale of variation of  $(\hat{f}_K, \hat{\phi}_K)$  is of the order  $\epsilon$ , i.e.,

$$\hat{f}_K = \hat{f}_K(\eta, \zeta_y, \zeta_2, \zeta_3), \quad \hat{\phi}_K = \hat{\phi}_K(\eta), \tag{33}$$

or  $\partial \hat{f}_K / \partial \eta = O(\hat{f}_K)$  and  $d\hat{\phi}_K / d\eta = O(\hat{\phi}_K)$ , and that  $(\hat{f}_K, \hat{\phi}_K)$  vanishes rapidly as  $\eta \rightarrow \infty$ . We further suppose that  $(\hat{f}_K, \hat{\phi}_K)$  is expanded in  $\epsilon$  as

$$\hat{f}_K = \hat{f}_{K1}\epsilon + \hat{f}_{K2}\epsilon^2 + \dots, \tag{34}$$

$$\hat{\phi}_K = \hat{\phi}_{K1}\epsilon + \hat{\phi}_{K2}\epsilon^2 + \dots. \tag{35}$$

Corresponding to (31, 32, 34), and (35), the macroscopic quantity  $h$  (where  $h = \hat{\rho}, \hat{J}, \hat{u}$ , or  $\hat{T}$ ) and the electric field  $\hat{E}$  are expressed as

$$h = h_H + h_K, \tag{36}$$

$$\hat{E} = \hat{E}_H + \hat{E}_K, \tag{37}$$

with

$$h_K = h_{K1}\epsilon + h_{K2}\epsilon^2 + \dots, \tag{38}$$

$$\hat{E}_K = \hat{E}_{K0} + \hat{E}_{K1}\epsilon + \hat{E}_{K2}\epsilon^2 + \dots. \tag{39}$$

Here, the expansion of  $\hat{E}_K$  starts from order  $\epsilon^0$  for the following reason. If we substitute (32) and (37) into (9) and take into account that  $\hat{E}_H$  and  $\hat{\phi}_H$  solve the equation, we obtain

$$\hat{E}_K = \mp \frac{1}{\epsilon} \frac{d\hat{\phi}_K}{d\eta}, \tag{40}$$

where the minus (plus) sign corresponds to the Knudsen layer around  $x_1 = 0$  ( $x_1 = 1$ ). This convention is used throughout the paper. Since  $\hat{\phi}_K = O(\epsilon)$  and  $d\hat{\phi}_K / d\eta = O(\hat{\phi}_K)$  [see the sentence that contains (33)], we conclude that  $\hat{E}_K = O(1)$  and therefore, the  $\hat{E}_{K0}$  term in the expansion (39) is not zero.

Substituting the expansions (35) and (39) into (40) and equating the coefficients of the same power of  $\epsilon$  yields the following expression of  $\hat{E}_{Km}$  in terms of  $\hat{\phi}_{Km}$ :

$$\hat{E}_{K m-1} = \mp \frac{d\hat{\phi}_{Km}}{d\eta} \quad (m \geq 1). \tag{41}$$

In order to obtain the relation between  $h_{Km}$  and  $\hat{f}_{Km}$ , we substitute (31) [with (15) and (34)] and (36) [with (17) and (38)] into (7, 13), and (14) and take into account the

relation between  $h_{Hm}$  and  $\hat{f}_{Hm}$  [e.g., (19, 20)]. Thus, for  $\hat{\rho}_{Km}$  and  $\hat{J}_{Km}$ , we obtain the expressions

$$\hat{\rho}_{Km} = \int \hat{f}_{Km} d^3\bar{\zeta}, \quad \hat{J}_{Km} = \int \zeta_1 \hat{f}_{Km} d^3\bar{\zeta}, \tag{42}$$

where  $d^3\bar{\zeta} = d\zeta_1 d\zeta_2 d\zeta_3$ . We omit the result for  $\hat{u}_{Km}$  and  $\hat{T}_{Km}$  for brevity.

To derive the equations for  $(\hat{f}_K, \hat{\phi}_K)$ , we substitute (31, 32) and (36) (with  $h = \hat{\rho}$ ) together with their expansions into (6) [with (9)] and (8), and use the Taylor expansion for  $(\hat{f}_K, \hat{\phi}_K)$  and  $\hat{\tau}$  near the boundary. This yields a sequence of equations for  $(\hat{f}_{Km}, \hat{\phi}_{Km})$  ( $m \geq 1$ ). On the other hand, the boundary conditions for  $(\hat{f}_{Km}, \hat{\phi}_{Km})$  are derived from the requirements  $(\hat{f}_{Hm})_B + (\hat{f}_{Km})_B = 0$  (for  $\zeta_y > 0$ ) and  $(\hat{\phi}_H)_B + (\hat{\phi}_{Km})_B = 0$  on the boundary, where  $(\cdot)_B$  denotes the value on the boundary. Furthermore, the condition  $(\hat{f}_{Km}, \hat{\phi}_{Km}) \rightarrow (0, 0)$  as  $\eta \rightarrow \infty$  needs to be imposed. In the following, we present the explicit equations and boundary conditions for  $(\hat{f}_{K1}, \hat{\phi}_{K1})$  and  $(\hat{f}_{K2}, \hat{\phi}_{K2})$  thus obtained:

$$\zeta_y \frac{\partial \hat{f}_{Km}}{\partial \eta} + \frac{1}{2} \frac{d\hat{\phi}_{Km}}{d\eta} \frac{\partial}{\partial \zeta_y} (\hat{f}_{H0})_B = \frac{1}{(\hat{\tau})_B} (\hat{\rho}_{Km} \mathcal{M} - \hat{f}_{Km}) + I_m, \tag{43}$$

$$\lambda^2 \frac{d^2 \hat{\phi}_{Km}}{d\eta^2} = 0, \tag{44}$$

$$\hat{f}_{Km} = -\mathcal{M} [(\hat{\rho}_{Hm})_B + L_m] \quad (\text{for } \zeta_y > 0), \tag{45}$$

$$\hat{\phi}_{Km} = -(\hat{\phi}_{Hm})_B \tag{46}$$

at  $\eta = 0$ , and

$$\hat{f}_{Km} \rightarrow 0, \quad \hat{\phi}_{Km} \rightarrow 0 \tag{47}$$

as  $\eta \rightarrow \infty$ . Here,  $m = 1, 2$ , and  $I_m$  and  $L_m$  are given by

$$I_1 = 0, \tag{48a}$$

$$I_2 = -\frac{1}{2} \left( \frac{d\hat{\phi}_{H0}}{dy} \right)_B \frac{\partial \hat{f}_{K1}}{\partial \zeta_y} + \frac{d\hat{\phi}_{K1}}{d\eta} \frac{\partial}{\partial \zeta_y} \left[ (\hat{f}_{H1})_B + \left( \frac{d\hat{f}_{H0}}{dy} \right)_B \eta + \hat{f}_{K1} \right] - \frac{1}{(\hat{\tau})_B^2} \left( \frac{d\hat{\tau}}{dy} \right)_B \eta (\hat{\rho}_{K1} \mathcal{M} - \hat{f}_{K1}), \tag{48b}$$

$$L_1 = 2(\tilde{J}_{H1})_B \zeta_y, \tag{48c}$$

$$L_2 = 2(\tilde{J}_{H2})_B \zeta_y + 2(\hat{\tau})_B \left( \frac{d\hat{\phi}_{H0}}{dy} \right)_B (\tilde{J}_{H1})_B \left( \zeta_y^2 - \frac{1}{2} \right), \tag{48d}$$

where

$$\tilde{J}_{H1} = -\frac{1}{2} \hat{\tau} \left( \frac{d\hat{\rho}_{H0}}{dy} - \hat{\rho}_{H0} \frac{d\hat{\phi}_{H0}}{dy} \right), \tag{49}$$

$$\tilde{J}_{H2} = -\frac{1}{2} \hat{\tau} \left( \frac{d\hat{\rho}_{H1}}{dy} - \hat{\rho}_{H0} \frac{d\hat{\phi}_{H1}}{dy} - \hat{\rho}_{H1} \frac{d\hat{\phi}_{H0}}{dy} \right). \tag{50}$$

We observe that the equations and boundary conditions for  $\hat{\phi}_{Km}$  ( $m = 1, 2$ ), i.e., (44, 46), and (47), are in closed form. Therefore, we first consider the problem for  $\hat{\phi}_{Km}$ . We claim

that  $(\hat{\phi}_{Hm})_B$  vanishes. Indeed, integrating (44) and employing the condition (47), we find  $\hat{\phi}_{Km} = 0$  for all  $\eta \geq 0$ . Therefore, in order for the boundary-value problem to have a solution,  $(\hat{\phi}_{Hm})_B$  in (46) must satisfy  $(\hat{\phi}_{Hm})_B = 0$  ( $m = 1, 2$ ). This gives the boundary condition for the second equation in (27c) and (28c). Moreover, it implies, by (41) that  $\hat{E}_{K0} = \hat{E}_{K1} = 0$ .

Next, we consider the problem for  $\hat{f}_{Km}$  ( $m = 1, 2$ ). Let us introduce the following variables:

$$\Phi_{Km} = \frac{\hat{f}_{Km}}{\mathcal{M}}, \quad \eta' = \frac{\eta}{(\hat{\tau})_B}, \quad y' = \frac{y}{(\hat{\tau})_B}.$$

Then the equation and boundary conditions for  $\hat{f}_{Km}$ , (43, 45, 47), can be transformed into

$$\zeta_y \frac{\partial \Phi_{Km}}{\partial \eta'} = \hat{\rho}_{Km} - \Phi_{Km} + \mathcal{I}_m, \tag{51}$$

$$\Phi_{Km} = -(\hat{\rho}_{Hm})_B + \mathcal{L}_m \quad (\text{for } \zeta_y > 0, \text{ at } \eta' = 0), \tag{52}$$

$$\Phi_{Km} \rightarrow 0 \quad (\text{as } \eta' \rightarrow \infty), \tag{53}$$

where

$$\mathcal{I}_1 = 0, \tag{54a}$$

$$\mathcal{I}_2 = -\frac{1}{2} \left( \frac{d\hat{\phi}_{H0}}{dy'} \right)_B \left( \frac{\partial \Phi_{K1}}{\partial \zeta_y} - 2\zeta_y \Phi_{K1} \right) - \frac{1}{(\hat{\tau})_B} \left( \frac{d\hat{\tau}}{dy'} \right)_B \eta' (\hat{\rho}_{K1} - \Phi_{K1}), \tag{54b}$$

$$\mathcal{L}_1 = -2(\tilde{\mathcal{J}}_{H1})_B \zeta_y, \tag{54c}$$

$$\mathcal{L}_2 = -2(\tilde{\mathcal{J}}_{H1})_B \zeta_y - 2 \left( \frac{d\hat{\phi}_{H0}}{dy'} \right)_B (\tilde{\mathcal{J}}_{H1})_B \left( \zeta_y^2 - \frac{1}{2} \right). \tag{54d}$$

Equations (51–53) form a one-dimensional boundary-value problem (half-space problem) of the linear semiconductor Boltzmann equation with a relaxation-time collision operator. The problem is also called the Milne problem. Concerning the problem with more general  $\mathcal{I}_m$  and  $\mathcal{L}_m$ , the following statements holds: (i) For a given function  $\mathcal{I}_m(\eta', \zeta_y, \zeta_2, \zeta_3)$  which satisfies  $\int \mathcal{I}_m \mathcal{M} d^3 \zeta = 0$  and  $\mathcal{I}_m \rightarrow 0$  (rapidly) as  $\eta' \rightarrow 0$  and a given function  $\mathcal{L}_m(\eta', \zeta_y, \zeta_2, \zeta_3)$ , the solution  $\Phi_{Km}$  is determined together with the constant  $(\hat{\rho}_{Hm})_B$  contained in the boundary condition (52). (ii)  $\int \zeta_y \Phi_{Km} \mathcal{M} d^3 \zeta = 0$  holds [this is obvious from (51) and (53)]. The boundary value  $(\hat{\rho}_{Hm})_B$  thus determined gives the boundary condition for the fluid-dynamic equations (27a, b), (28a), and (28b). We mention that the property of the half-space problem described above has been proved for the linear semiconductor Boltzmann equation with a general collision operator in the homogeneous case (i.e.,  $\mathcal{I}_m = 0$ ) in [20]. It follows from (ii) and (42) that  $\hat{J}_{Km} = 0$  for  $m = 1, 2$ .

In view of the expressions for  $\mathcal{I}_m$  and  $\mathcal{L}_m$ , we can seek the solutions  $\Phi_{K1}$  and  $\Phi_{K2}$  in the form

$$\begin{bmatrix} \Phi_{K1} \\ (\hat{\rho}_{H1})_B \end{bmatrix} = \begin{bmatrix} \psi_1 \\ \xi_1 \end{bmatrix} (\tilde{\mathcal{J}}_{H1})_B, \tag{55}$$

$$\begin{aligned} \begin{bmatrix} \Phi_{K2} \\ (\hat{\rho}_{H2})_B \end{bmatrix} &= \begin{bmatrix} \psi_{2a} \\ \xi_{2a} \end{bmatrix} (\tilde{\mathcal{J}}_{H2})_B - \begin{bmatrix} \psi_{2b} \\ \xi_{2b} \end{bmatrix} \left( \frac{d\hat{\phi}_{H0}}{dy'} \right)_B (\tilde{\mathcal{J}}_{H1})_B \\ &\quad + \begin{bmatrix} \psi_{2c} \\ \xi_{2c} \end{bmatrix} \frac{1}{(\hat{\tau})_B} \left( \frac{d\hat{\tau}}{dy'} \right)_B (\tilde{\mathcal{J}}_{H1})_B, \end{aligned} \tag{56}$$

where  $\xi_1, \xi_{2a}, \xi_{2b}$ , and  $\xi_{2c}$  are constants to be determined together with the solutions. Each problem is analyzed numerically to determine  $(\xi_\alpha, \psi_\alpha)$  ( $\alpha = 1, 2a, 2b, 2c$ ). We refer to Appendix 2 for a brief comment on the numerical solution of this problem. Once we obtain  $(\xi_\alpha, \psi_\alpha)$  and thus  $\Phi_{K1}$  and  $\Phi_{K2}$ , the Knudsen-layer parts of the electron number density, the mean flow velocity, and the electron temperature are readily calculated.

Before presenting the boundary conditions and the Knudsen-layer parts of the fluid-dynamic equations (26a–28c), we comment on the second-order Knudsen-layer part of the electric field  $\hat{E}_{K2}$ . Since  $\hat{E}_{K2}$  is determined by  $\hat{\phi}_{K3}$  [see (41) with  $m = 3$ ], we need some information from the Knudsen-layer problem of order  $\epsilon^3$  in order to obtain  $\hat{E}_{K2}$ . Namely, the Knudsen-layer equation for  $\hat{\phi}_{K3}$  is given by

$$\lambda^2 \frac{d^2 \hat{\phi}_{K3}}{d\eta^2} = \hat{\rho}_{K1}.$$

Since  $\hat{\rho}_{K1}$  is already known from the lower order Knudsen-layer problem, integration of the above equation under the boundary condition  $\hat{\phi}_{K3} \rightarrow 0$  (as  $\eta \rightarrow \infty$ ) yields an expression of  $d\hat{\phi}_{K3}/d\eta$ . Then, (41) for  $m = 3$  immediately gives the desired formula for  $\hat{E}_{K2}$ . Incidentally, the integration of the Knudsen-layer equation for  $\hat{f}_{K3}$  with respect to  $(\zeta_y, \zeta_2, \zeta_3)$  over the whole space yields  $\hat{J}_{K3} = \int \zeta_1 \hat{f}_{K3} d\vec{\zeta} = 0$ . This relation (and the relation between  $\hat{u}_{K3}$  and  $\hat{f}_{K3}$ ) is used to derive the expression of  $\hat{u}_{K3}$  given in (61b) below. In general, from the analysis of the Knudsen-layer problem for  $(\hat{f}_{Km}, \hat{\phi}_{Km})$ , we obtain the boundary values  $(\hat{\rho}_{Hm})_B$  and  $(\hat{\phi}_{Hm})_B$  and the Knudsen-layer parts of  $\hat{\phi}_{Km}, h_{Km}$  ( $h = \hat{\rho}, \hat{J}, \hat{u}$ , or  $\hat{T}$ ), and  $\hat{E}_{Km-1}$ .

Finally, we summarize the boundary conditions for the fluid-dynamic equations and the computed Knudsen-layer parts. The boundary conditions for (27a–28c) are given by

$$\begin{aligned} (\hat{\rho}_{H1})_B &= \xi_1 (\tilde{J}_{H1})_B, & (\hat{\phi}_{H1})_B &= 0, & (57) \\ (\hat{\rho}_{H2})_B &= \xi_{2a} (\tilde{J}_{H2})_B - \xi_{2b} (\hat{\tau})_B \left( \frac{d\hat{\phi}_{H0}}{dy} \right)_B (\tilde{J}_{H1})_B + \xi_{2c} \left( \frac{d\hat{\tau}}{dy} \right)_B (\tilde{J}_{H1})_B, & & & (58) \\ (\hat{\phi}_{H2})_B &= 0, \end{aligned}$$

where the numerical values of the slip coefficients  $\xi_1, \xi_{2a}, \xi_{2b}$ , and  $\xi_{2c}$  are given by  $\xi_1 = \xi_{2a} = -2.03238284, \xi_{2b} = 1.03264500$ , and  $\xi_{2c} = 0$ . The Knudsen-layer parts are as follows. For  $m = 0$  we have  $\hat{E}_{K0} = 0$ ; for  $m = 1, \hat{\phi}_{K1} = \hat{E}_{K1} = \hat{J}_{K1} = \hat{u}_{K1} = 0$ ,

$$\hat{\rho}_{K1} = \Omega_1(\eta') (\tilde{J}_{H1})_B, \tag{59a}$$

$$\hat{T}_{K1} = -\frac{1}{3} \frac{(\tilde{J}_{H1})_B}{(\hat{\rho}_{H0})_B} \Omega_1(\eta'), \tag{59b}$$

for  $m = 2$ ,

$$\begin{aligned} \hat{\rho}_{K2} &= \Omega_1(\eta') (\tilde{J}_{H2})_B - [\Omega_2(\eta') + \Omega_3(\eta')] (\hat{\tau})_B \left( \frac{d\hat{\phi}_{H0}}{dy} \right)_B (\tilde{J}_{H1})_B \\ &+ \Omega_4(\eta') \left( \frac{d\hat{\tau}}{dy} \right)_B (\tilde{J}_{H1})_B, \end{aligned} \tag{60a}$$

$$\hat{T}_{K2} = -\frac{1}{3(\hat{\rho}_{H0})_B} \left\{ \Omega_1(\eta') (\tilde{J}_{H2})_B - \left[ \Omega_2(\eta') + \Omega_3(\eta') - \int_{\eta'}^{\infty} \Omega_1(s) ds \right] \right\}$$

$$\begin{aligned} & \times (\hat{\tau})_B \left( \frac{d\hat{\phi}_{H0}}{dy} \right)_B (\tilde{J}_{H1})_B + \Omega_4(\eta') \left( \frac{d\hat{\tau}}{dy} \right)_B (\tilde{J}_{H1})_B \\ & - \left[ (\hat{\rho}_{H1})_B + (\hat{\tau})_B \left( \frac{d\hat{\rho}_{H0}}{dy} \right)_B \eta' + \Omega_1(\eta') (\tilde{J}_{H1})_B \right] \frac{(\tilde{J}_{H1})_B}{(\hat{\rho}_{H0})_B} \Omega_1(\eta') \Big\}, \end{aligned} \tag{60b}$$

$$\hat{u}_{K2} = -\Omega_1(\eta') (\hat{u}_{H1})_B (\tilde{J}_{H1})_B / (\hat{\rho}_{H0})_B, \tag{60c}$$

$$\hat{E}_{K2} = \pm \frac{(\hat{\tau})_B}{\lambda^2} (\tilde{J}_{H1})_B \int_{\eta'}^{\infty} \Omega_1(s) ds, \tag{60d}$$

$$\hat{\phi}_{K2} = \hat{J}_{K2} = 0, \tag{60e}$$

and finally, for  $m = 3$ ,

$$\hat{J}_{K3} = 0, \tag{61a}$$

$$\begin{aligned} \hat{u}_{K3} = & -\Omega_1(\eta') \frac{(\hat{u}_{H1})_B}{(\hat{\rho}_{H0})_B} \left\{ (\tilde{J}_{H2})_B - \left[ \frac{(\hat{\rho}_{H1})_B}{(\hat{\rho}_{H0})_B} - \frac{(\hat{u}_{H2})_B}{(\hat{u}_{H1})_B} + 2(\hat{\tau})_B \left( \frac{d \ln \hat{\rho}_{H0}}{dy} \right)_B \right] (\tilde{J}_{H1})_B \right\} \\ & + [\Omega_2(\eta') + \Omega_3(\eta')] (\hat{\tau})_B \left( \frac{d\hat{\phi}_{H0}}{dy} \right)_B \frac{(\hat{u}_{H1})_B}{(\hat{\rho}_{H0})_B} (\tilde{J}_{H1})_B \\ & - \Omega_4(\eta') \left( \frac{d\hat{\tau}}{dy} \right)_B \frac{(\hat{u}_{H1})_B}{(\hat{\rho}_{H0})_B} (\tilde{J}_{H1})_B + (\hat{u}_{H1})_B \left[ \frac{(\tilde{J}_{H1})_B}{(\hat{\rho}_{H0})_B} \Omega_1(\eta') \right]^2. \end{aligned} \tag{61b}$$

The values of the so-called Knudsen-layer functions  $\Omega_m(\eta')$  ( $m = 1, 2, 3, 4$ ) as well as those of the integral  $\int_{\eta'}^{\infty} \Omega_1(s) ds$  are displayed in Table 1.

### 4 Numerical Simulation of the Electron Flow in an $n^+nn^+$ Diode for Small Knudsen Numbers

In this section, we consider an electron flow induced in a semiconductor with a doping profile corresponding to a one-dimensional  $n^+nn^+$  diode. We make a numerical comparison between the asymptotic solution of the fluid-dynamic system obtained in the previous section and the direct numerical solution of the Boltzmann–Poisson system.

#### 4.1 Comments on the Numerical Method

The similarity between the present relaxation-time semiconductor Boltzmann equation and the Boltzmann equation for rarefied gases with relaxation collision terms, like the BGK model [34–36], allows us to employ numerical techniques developed for the BGK-Boltzmann equation in order to solve the semiconductor problem. For example, we can eliminate the independent variables  $\zeta_2$  and  $\zeta_3$  from the system (see [37]). For this, let us introduce a function (the so-called marginal velocity distribution function)  $\mathcal{G}(x_1, \zeta_1)$  by

$$\mathcal{G}(x_1, \zeta_1) = \int_{-\infty}^{\infty} \int_{-\infty}^{\infty} \hat{f} d\zeta_2 d\zeta_3.$$

Integrating (6) with respect to  $\zeta_2$  and  $\zeta_3$  over the whole range of the variables gives a system of equations for  $(\mathcal{G}, \hat{\phi})$ . The corresponding boundary conditions for  $\mathcal{G}$  are obtained from (11)

**Table 1** Knudsen-layer functions. The Knudsen-layer functions generally have the singularity  $\eta' \ln \eta'$  at  $\eta' = 0$ . Their coefficients are also shown

$\eta'$	$\Omega_1$	$-\Omega_2$	$\Omega_3$	$\Omega_4$	$\int_{\eta'}^{\infty} \Omega_1(s) ds$
0.00	0.61817	1.09553	0.78144	0.00000	0.46736
0.05	0.51453	0.96234	0.68806	0.00174	0.43948
0.10	0.45655	0.87923	0.62444	0.00492	0.41529
0.20	0.37755	0.75753	0.52794	0.01288	0.37386
0.40	0.28006	0.59357	0.39526	0.02996	0.30898
0.60	0.21858	0.48163	0.30500	0.04557	0.25951
0.80	0.17546	0.39864	0.23931	0.05876	0.22034
1.00	0.14349	0.33441	0.18975	0.06948	0.18859
1.20	0.11895	0.28333	0.15152	0.07790	0.16245
1.40	0.09965	0.24193	0.12154	0.08429	0.14066
1.60	0.08418	0.20788	0.09776	0.08892	0.12234
1.80	0.07160	0.17956	0.07874	0.09205	0.10680
2.00	0.06127	0.15580	0.06341	0.09392	0.09355
2.50	0.04235	0.11103	0.03657	0.09440	0.06799
3.00	0.02996	0.08056	0.02041	0.09079	0.05012
4.00	0.01574	0.04413	0.00464	0.07770	0.02813
5.00	0.00867	0.02512	-0.00097	0.06263	0.01631
6.00	0.00494	0.01471	-0.00263	0.04878	0.00969
8.00	0.00173	0.00537	-0.00242	0.02798	0.00361
10.00	0.00065	0.00208	-0.00148	0.01543	0.00142
12.00	0.00026	0.00084	-0.00082	0.00835	0.00059
coeff. of $\eta' \ln \eta'$	0.79788	0.81080	0.40540	0	0

and (12) in a similar way. The resulting system for  $(\mathcal{G}, \hat{\phi})$  is given by

$$\zeta_1 \frac{\partial \mathcal{G}}{\partial x_1} - \frac{1}{2} \hat{E} \frac{\partial \mathcal{G}}{\partial \zeta_1} = \frac{2}{\sqrt{\pi} \text{Kn}} \frac{1}{\hat{t}} \left( \frac{\hat{\rho} e^{-\zeta_1^2}}{\pi^{1/2}} - \mathcal{G} \right), \quad \hat{\rho} = \int_{-\infty}^{\infty} \mathcal{G} d\zeta_1, \tag{62}$$

$$\lambda^2 \frac{d^2 \hat{\phi}}{dx_1^2} = \hat{\rho} - \hat{C}, \quad \hat{E} = -\frac{d\hat{\phi}}{dx_1}, \tag{63}$$

with the boundary conditions

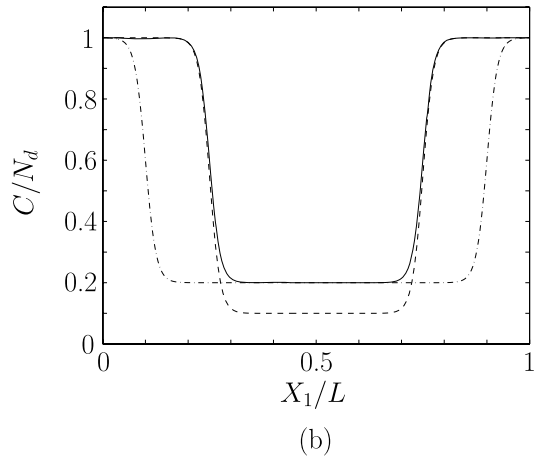
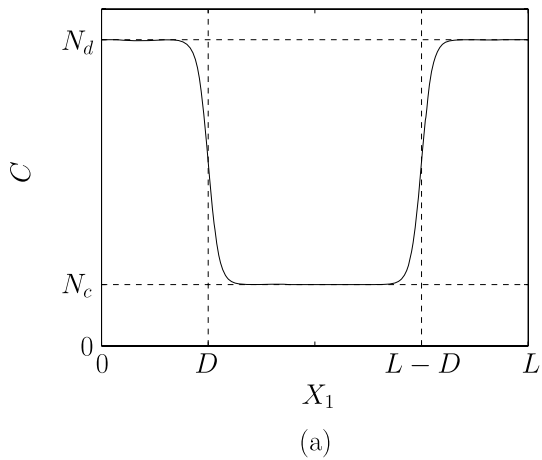
$$\mathcal{G} = \frac{\hat{C}(0)}{\pi^{1/2}} \exp(-\zeta_1^2) \quad \text{for } \zeta_1 > 0, \quad \hat{\phi} = \hat{\phi}_A \text{ at } x_1 = 0, \tag{64}$$

$$\mathcal{G} = \frac{\hat{C}(1)}{\pi^{1/2}} \exp(-\zeta_1^2) \quad \text{for } \zeta_1 < 0, \quad \hat{\phi} = \hat{\phi}_B \text{ at } x_1 = 1. \tag{65}$$

The system (62–65) is solved numerically by a finite difference method similar to that used in [38] but including an additional step to solve the Poisson equation.

It should be noted that  $\hat{T}$  cannot be expressed in terms of  $\mathcal{G}$  alone [cf. (14)]. In order to compute  $\hat{T}$ , we introduce, in addition to  $\mathcal{G}$ , the marginal velocity distribution function  $\mathcal{H} = \int_{-\infty}^{\infty} \int_{-\infty}^{\infty} (\zeta_2^2 + \zeta_3^2) \hat{f} d\zeta_2 d\zeta_3$ . The equation and the boundary conditions for  $\mathcal{H}$  are ob-

**Fig. 1** (a) The doping profile  $C$ . (b) The doping profile  $C$  normalized by  $N_d$  with  $N_c/N_d = 0.2, D/L = 0.25$  (solid line);  $N_c/N_d = 0.2, D/L = 0.1$  (dash-dotted line);  $N_c/N_d = 0.1, D/L = 0.25$  (dashed line)



tained in the same way as those for  $\mathcal{G}$ . It turns out that the form of the equation and boundary condition for  $\mathcal{H}$  coincides with that for  $\mathcal{G}$ , and therefore,  $\mathcal{H} = \mathcal{G}$  holds. Thus, we can compute  $\hat{T}$  from the solution  $\mathcal{G}$ .

#### 4.2 Numerical Results

The semiconductor device is specified by the doping profile  $C(X_1)$  and the relaxation time  $\tau(X_1)$ . We choose

$$C(X_1) = N_d + \frac{N_d - N_c}{2} \left[ \tanh\left(40 \frac{X_1 - L + D}{L}\right) - \tanh\left(40 \frac{X_1 - D}{L}\right) \right],$$

[see Fig. 1(a)] modeling an  $n^+nn^+$  diode. Here, the positive constants  $N_d, N_c (< N_d)$ , and  $D (< L/2)$  denote the doping concentration of the highly doped ( $n^+$ ) region, that of the channel ( $n$ ) region, and the position of the junctions (the doping profile is symmetric with respect to  $X_1 = L/2$ ), respectively. The relaxation time is assumed to be constant,  $\tau = \tau_0$ , such that  $\hat{\tau} = 1$ .

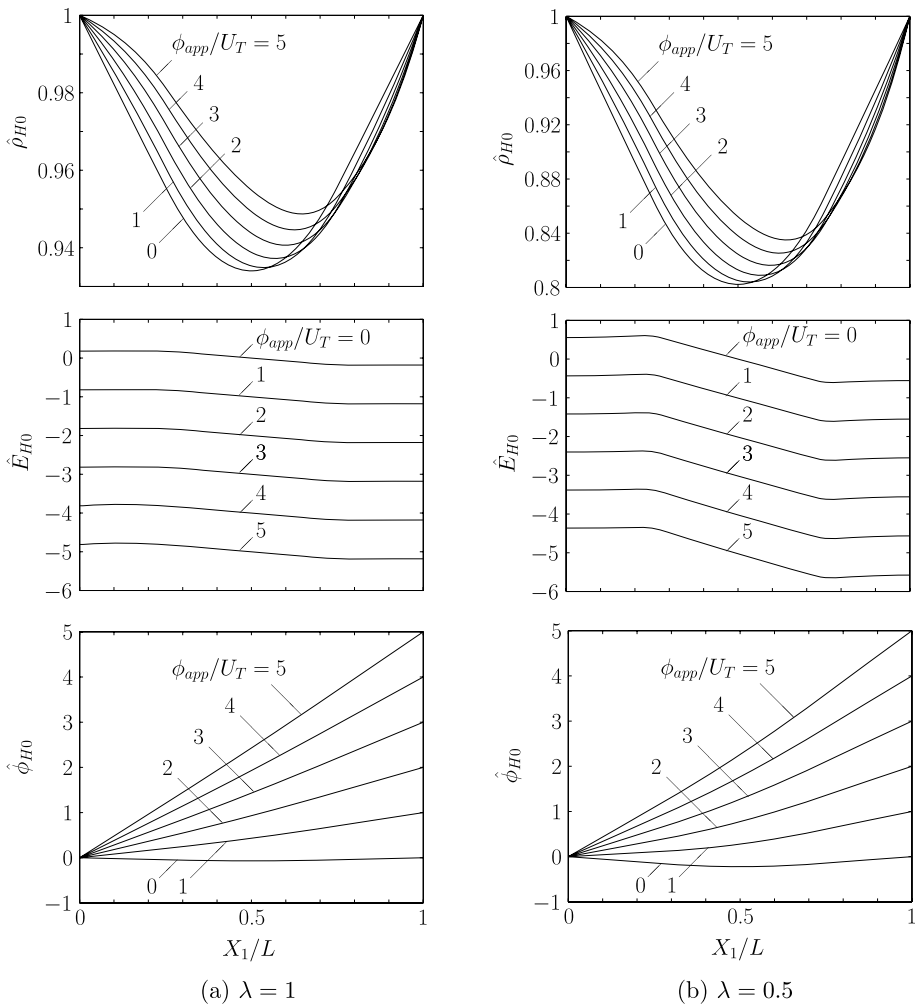


**Fig. 2** The solution  $\hat{\rho}_{H0}$ ,  $\hat{E}_{H0}$ , and  $\hat{\phi}_{H0}$  for various applied potentials  $\phi_{app}$  with  $N_c/N_d = 0.2$ ,  $D/L = 0.25$ , and (a)  $\lambda = 1$ , (b)  $\lambda = 0.5$

We take  $N_d$  as the reference value of the electron number density, i.e.,  $\rho_0 = N_d$  (see the first sentence of Sect. 2.3). The present problem is then characterized by the following parameters:  $\text{Kn}$ ,  $\lambda$ ,  $(\phi_B - \phi_A)/U_T$ ,  $\phi_B/U_T$ ,  $N_c/N_d$ , and  $D/L$ . For convenience, we introduce  $\phi_{app} = \phi_B - \phi_A$ .

We first present some numerical results for a doping profile with  $N_c/N_d = 0.2$  and  $D/L = 0.25$  [the solid line in Fig. 1(b)]. Figures 2–4 show the solutions of the fluid-dynamic equations (26a–28c) under the boundary conditions (29, 30, 57), and (58) for various values of  $\phi_{app}$  and for  $\lambda = 1$  and  $\lambda = 0.5$ .

Once we obtain  $\hat{\rho}_{Hm}$ ,  $\hat{E}_{Hm}$ , and  $\hat{\phi}_{Hm}$ , the asymptotic solution is readily obtained from (36, 37, 32, 17, 18, 16, 38, 39), and (35) by specifying  $\epsilon$  (or  $\text{Kn}$ ). The result is shown in Figs. 5 and 6 for  $\phi_{app}/U_T = 1$  and 3 in the cases  $\lambda = 1$  (Fig. 5) and  $\lambda = 0.5$  (Fig. 6), where the asymptotic solution of  $u$  (up to order  $\text{Kn}^3$ ) and that of  $T$



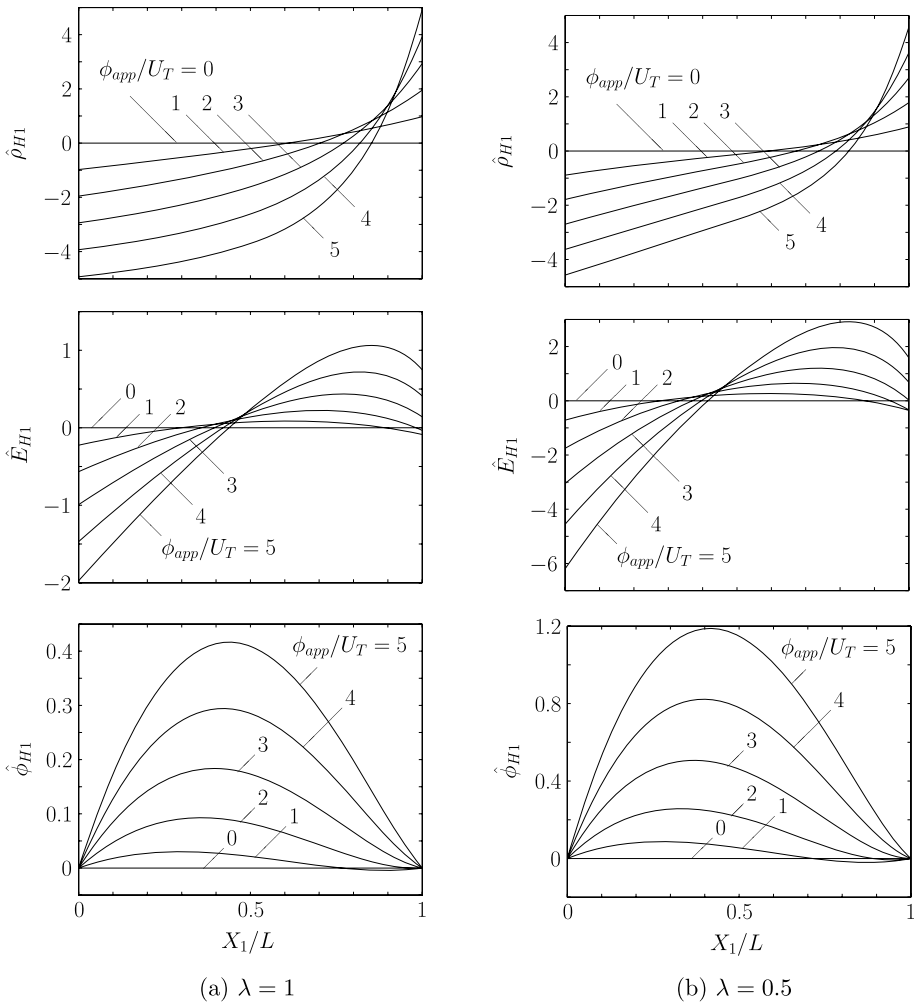


**Fig. 3** The solution  $\hat{\rho}_{H1}$ ,  $\hat{E}_{H1}$ , and  $\hat{\phi}_{H1}$  for various applied potentials  $\phi_{app}$  with  $N_c/N_d = 0.2$ ,  $D/L = 0.25$ , and (a)  $\lambda = 1$ , (b)  $\lambda = 0.5$

(up to order  $Kn^2$ ) are also included [the corresponding Hilbert solutions are obtained from  $\hat{\rho}_{Hm}$  and  $\hat{E}_{Hm}$  ( $m = 0, 1, 2$ ) with the aid of the formulas given in Appendix 1]. In Figs. 5 and 6, the direct numerical solutions of the original Boltzmann–Poisson system (6–9, 11–12) are also shown.

The numerical results show that the asymptotic solutions are in good agreement with the direct numerical solutions of the Boltzmann–Poisson system. However, there are some appreciable differences in the case  $Kn = 0.1$ . The difference increases with the applied potentials  $\phi_{app}$  and is more pronounced at the right boundary. This can be explained as follows.

First, the values of  $\hat{\rho}_{H1}$  and  $\hat{\rho}_{H2}$  as well as their gradients near  $X_1 = L$  are increasing in  $\phi_{app}/U_T$ . This results in a large value of  $\hat{u}_{H2}$  and  $\hat{u}_{H3}$  [see (68) and (69)]. Second, the second-order Knudsen-layer correction contains product terms depending on  $(d\hat{\phi}_{H0}/dy)_B$ ,

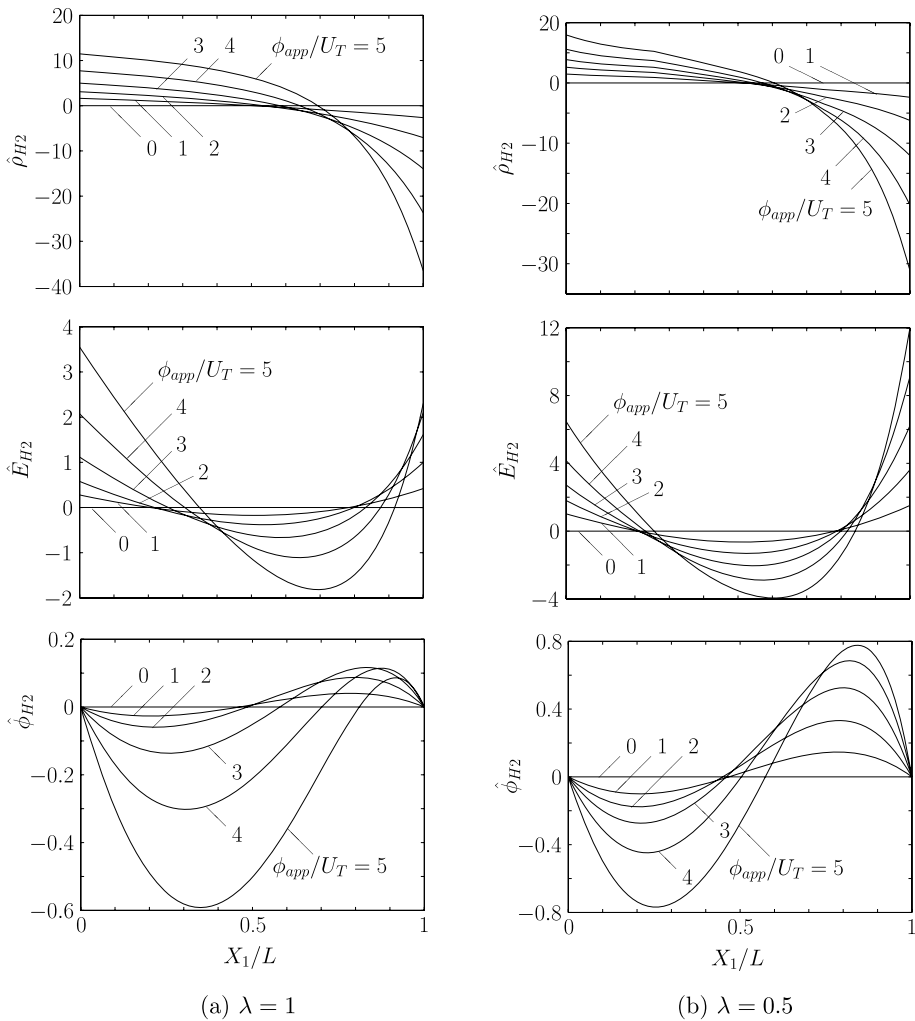


**Fig. 4** The solution  $\hat{\rho}_{H2}$ ,  $\hat{E}_{H2}$ , and  $\hat{\phi}_{H2}$  for various applied potentials  $\phi_{app}$  with  $N_c/N_d = 0.2$ ,  $D/L = 0.25$ , and **(a)**  $\lambda = 1$ , **(b)**  $\lambda = 0.5$

$(\tilde{J}_{H1})_B$ , and  $(\hat{u}_{H1})_B$  which are increasing in  $\phi_{app}/U_T$ . Therefore, the Knudsen-layer part for  $Kn = 0.1$  is not well confined near the boundary.

In Figs. 7 and 8, the current-voltage characteristics obtained from the numerical solution of the Boltzmann-Poisson system for various  $Kn$  at two values of  $\lambda$ , i.e.,  $\lambda = 1$  and  $0.5$ . For the doping profile we choose again  $N_c/N_d = 0.2$  and  $D/L = 0.25$ .

In the figures, we have included not only the asymptotic solution up to the order  $Kn^3$ , i.e.  $\hat{J}^{(3)} = \hat{J}_{H1}\epsilon + \hat{J}_{H2}\epsilon^2 + \hat{J}_{H3}\epsilon^3$ , but also the asymptotic solutions up to first and second order,  $\hat{J}^{(1)} = \hat{J}_{H1}\epsilon$  and  $\hat{J}^{(2)} = \hat{J}_{H1}\epsilon + \hat{J}_{H2}\epsilon^2$ , for comparison.  $\hat{J}^{(1)}$  and  $\hat{J}^{(2)}$  correspond to the current densities obtained from the conventional drift-diffusion system by applying the non-slip boundary condition and the boundary condition derived by Yamnahakki, respectively. As seen from the figures, the current density  $\hat{J}^{(3)}$  gives a result much closer to

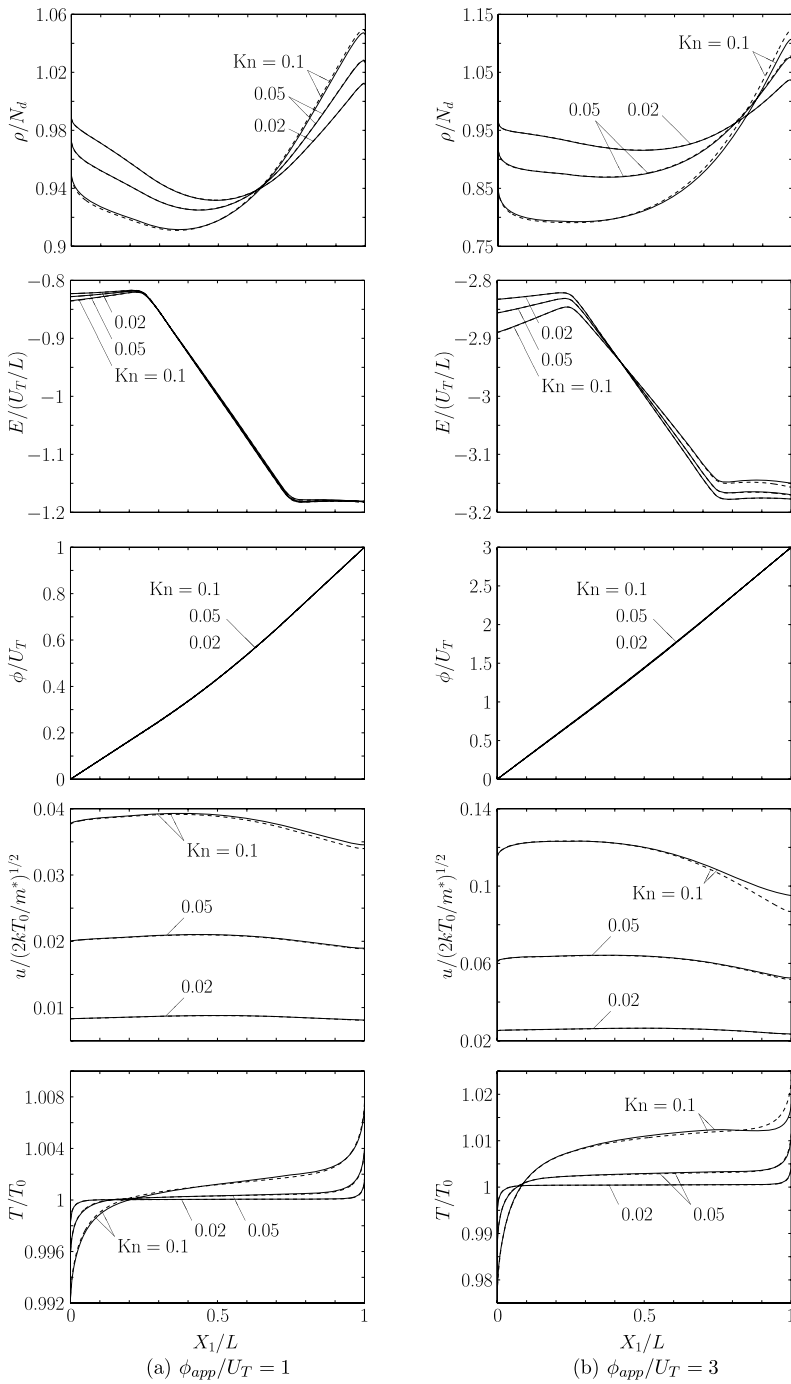


**Fig. 5** The profiles of the electron density  $\rho$ , electric field  $E$ , electrostatic potential  $\phi$ , mean flow velocity  $u$ , and electron temperature  $T$  for  $\text{Kn} = 0.1, 0.05$ , and  $0.02$  with  $\lambda = 1$ ,  $N_c/N_d = 0.2$ , and  $D/L = 0.25$ . The *solid line* indicates the asymptotic solution up to order  $\text{Kn}^2$  (up to order  $\text{Kn}^3$  in the case of  $u$ ), and the *dashed lines* indicate the corresponding numerical solutions of the original Boltzmann–Poisson system

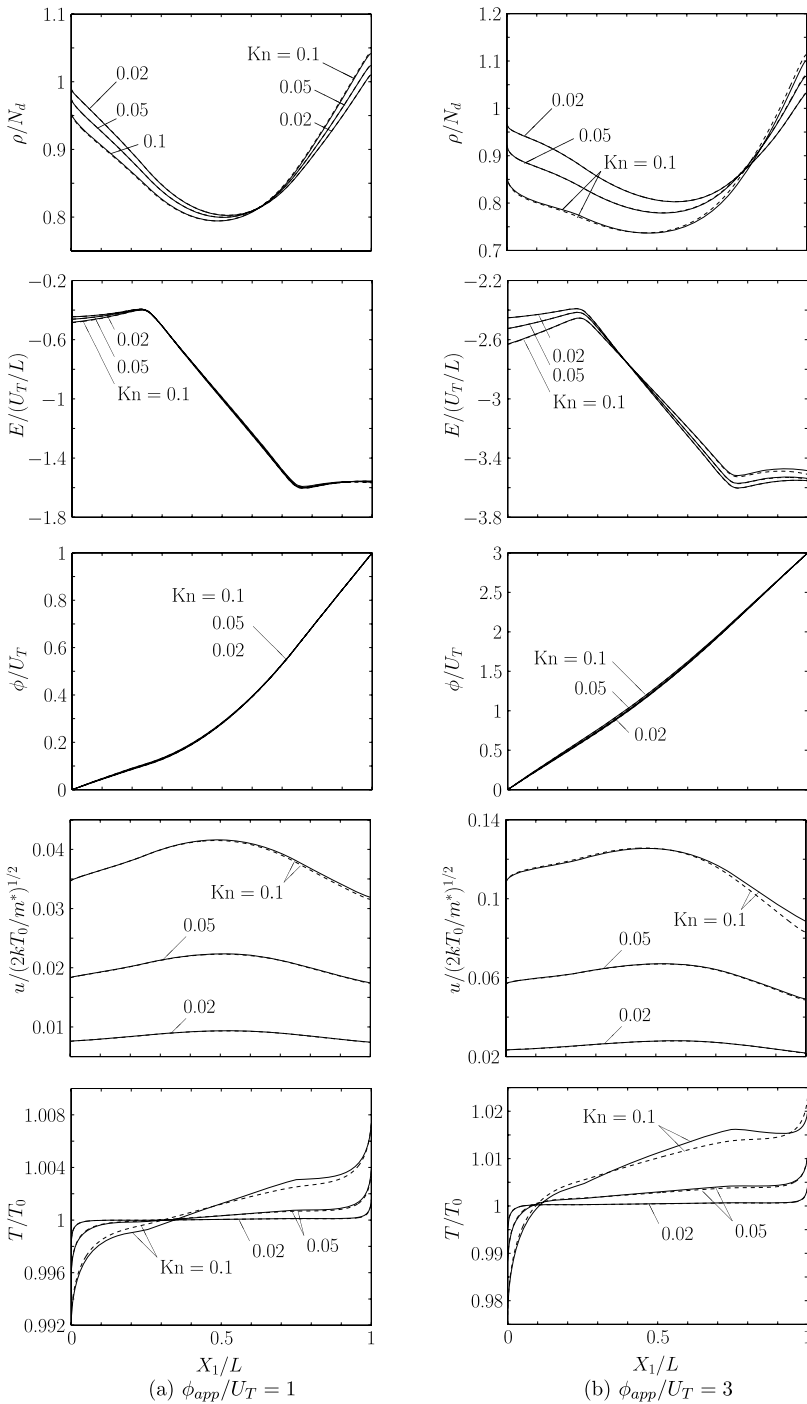
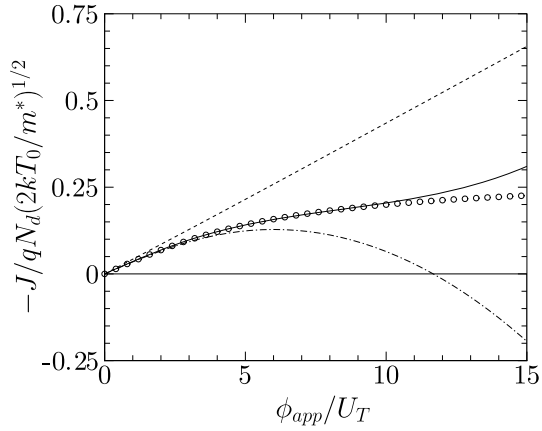
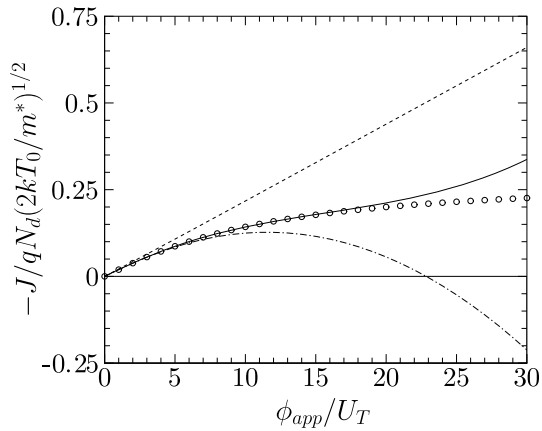


**Fig. 6** The profiles of the electron density  $\rho$ , electric field  $E$ , electrostatic potential  $\phi$ , mean flow velocity  $u$ , and electron temperature  $T$  for  $Kn = 0.1, 0.05,$  and  $0.02$  with  $\lambda = 0.5, N_c/N_d = 0.2,$  and  $D/L = 0.25$ . See the caption of Fig. 5

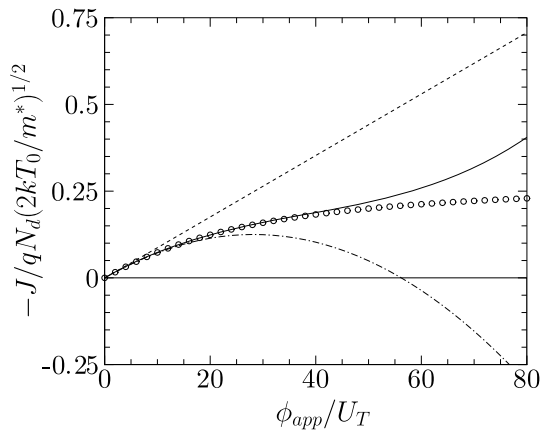
**Fig. 7** Current density  $J$  versus applied potential  $\phi_{app}$  for various  $\text{Kn}$  with  $\lambda = 1$ ,  $N_c/N_d = 0.2$ , and  $D/L = 0.25$ . The asymptotic solutions up to order  $\text{Kn}^3$  (solid line),  $\text{Kn}^2$  (dashed line), and  $\text{Kn}$  (dash-dotted line) are shown. The direct numerical solution of the Boltzmann–Poisson system is indicated by the symbol “o”. The line  $J = 0$  is also shown for convenience



(a)  $\text{Kn} = 0.1$

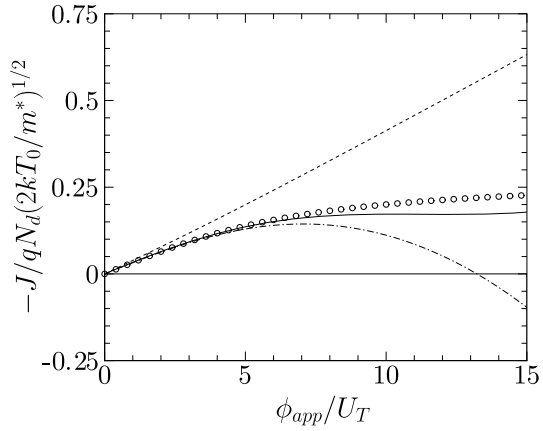


(b)  $\text{Kn} = 0.05$

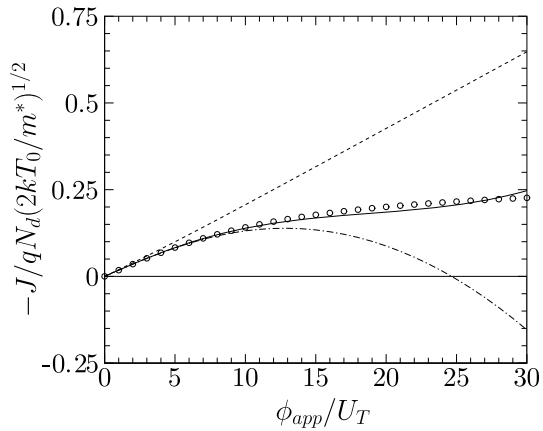


(c)  $\text{Kn} = 0.02$

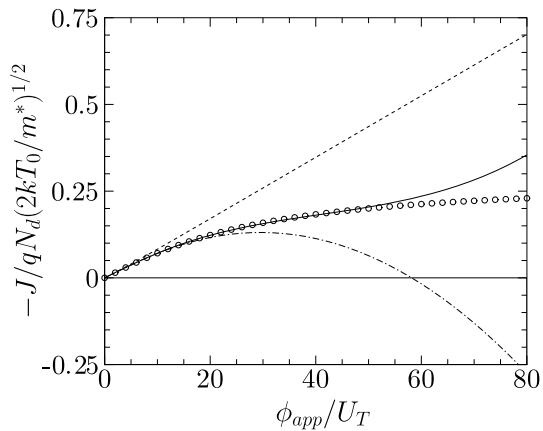
**Fig. 8** Current density  $J$  versus applied potential  $\phi_{app}$  for various Kn with  $\lambda = 0.5$ ,  $N_c/N_d = 0.2$ , and  $D/L = 0.25$ . See the caption of Fig. 7



(a) Kn = 0.1



(b) Kn = 0.05



(c) Kn = 0.02

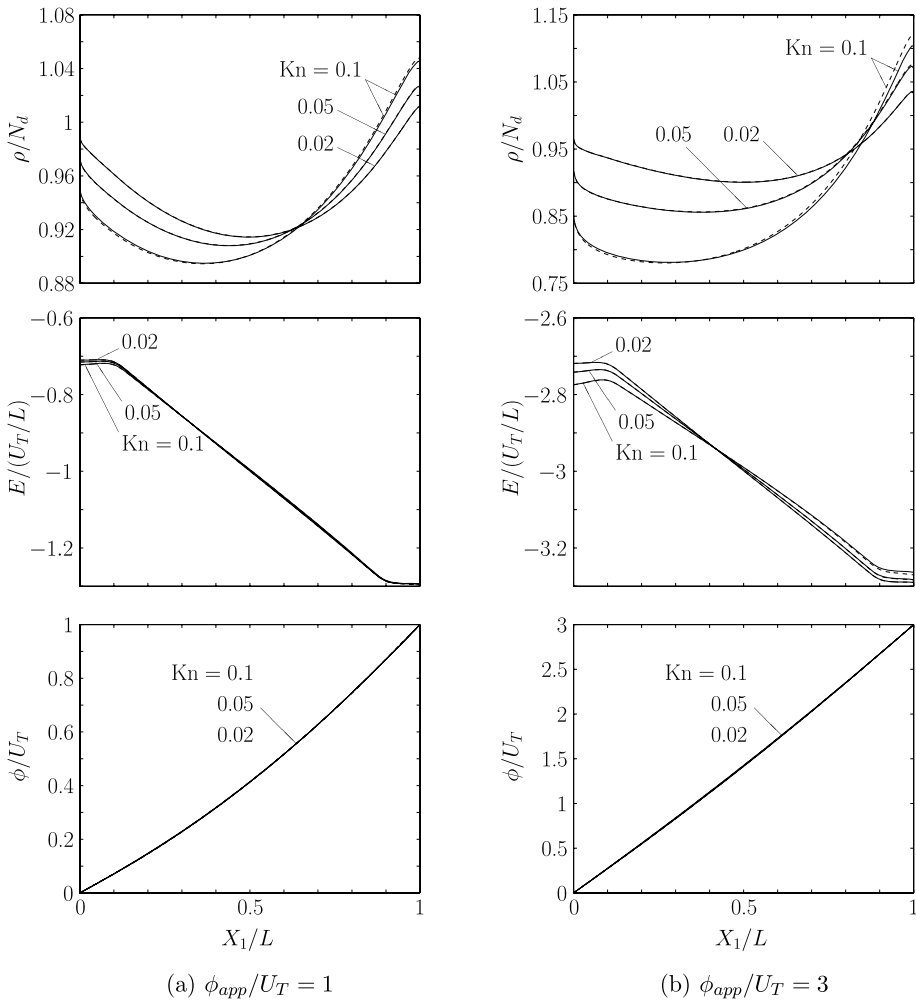


**Fig. 9** The profiles of the electron density  $\rho$ , electric field  $E$ , electrostatic potential  $\phi$  for  $Kn = 0.1, 0.05,$  and  $0.02$  with  $\lambda = 1, N_c/N_d = 0.2,$  and  $D/L = 0.1$ . The *solid line* indicates the asymptotic solution up to the order  $Kn^2$  and the *dashed line* the numerical solution of the original Boltzmann–Poisson system

the current-voltage characteristic obtained from the Boltzmann–Poisson system than  $\hat{J}^{(1)}$  and  $\hat{J}^{(2)}$ . The range of the applied potential where  $\hat{J}^{(3)}$  agrees well becomes larger when the Knudsen number becomes smaller. This is explained as follows. When the applied potential is increased, some electrons acquire velocities much faster than the thermal velocity in the direction parallel to the electric field, due to the strong electric field, resulting in long free paths. Therefore, for a large applied potential, the effective Knudsen number is no longer small, and the drift-diffusion approximation loses its accuracy. This effect is less pronounced for the small Knudsen numbers, since the effective Knudsen number remains small even when a large applied potential is applied. Hence, the range of applied potentials in which the drift-diffusion systems are accurate becomes larger for smaller Knudsen number.

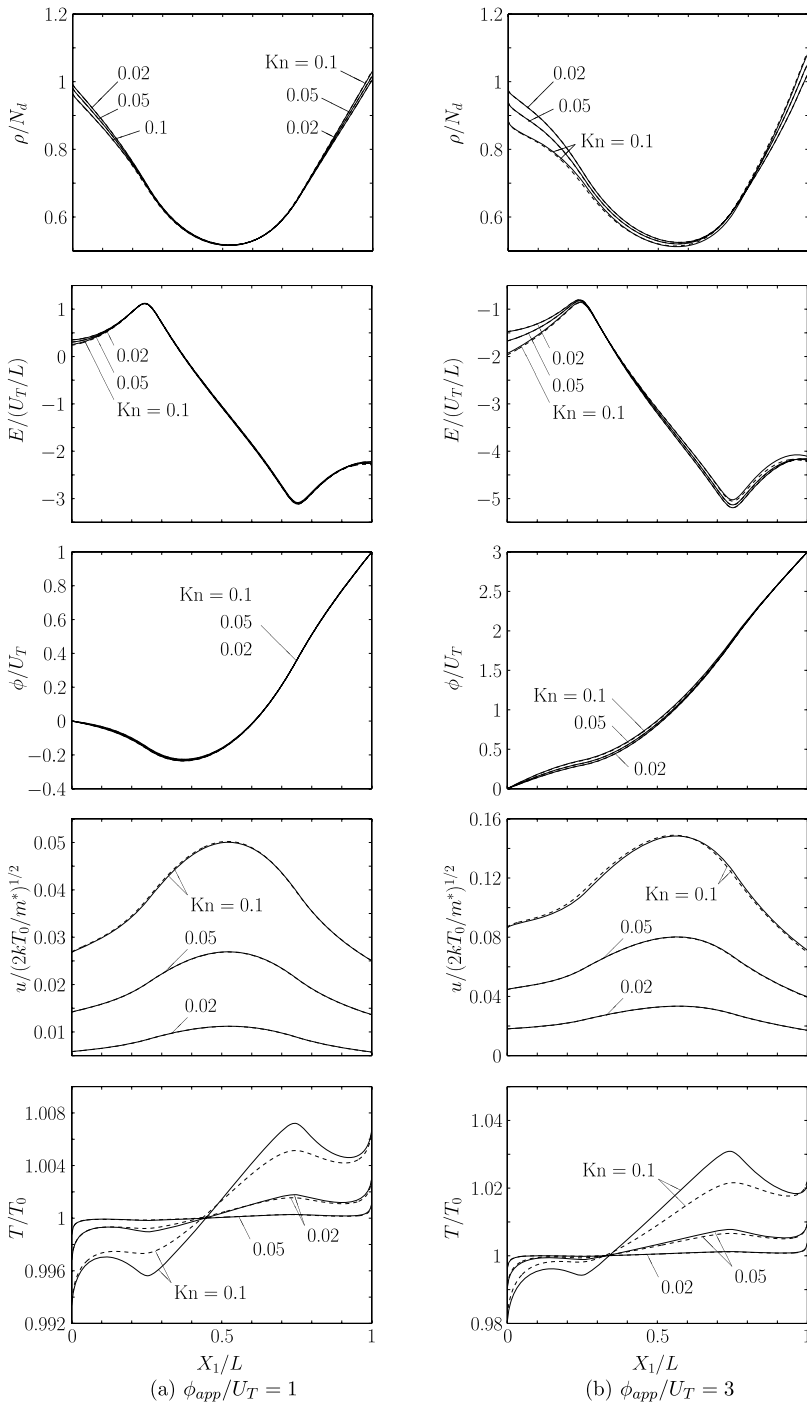
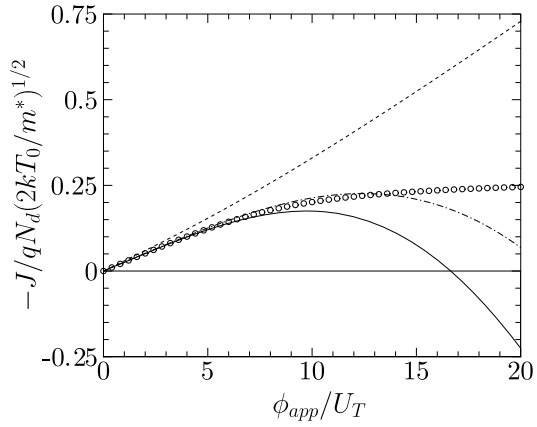


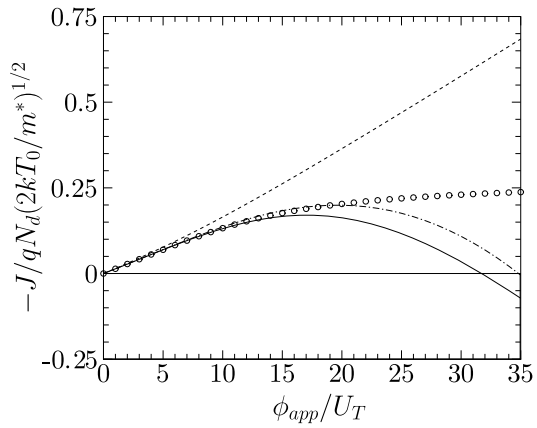
**Fig. 10** The profiles of the electron density  $\rho$ , electric field  $E$ , electrostatic potential  $\phi$ , mean flow velocity  $u$ , and electron temperature  $T$  for  $Kn = 0.1, 0.05$ , and  $0.02$  with  $\lambda = 0.2, N_c/N_d = 0.2$ , and  $D/L = 0.25$ . See the caption of Fig. 5



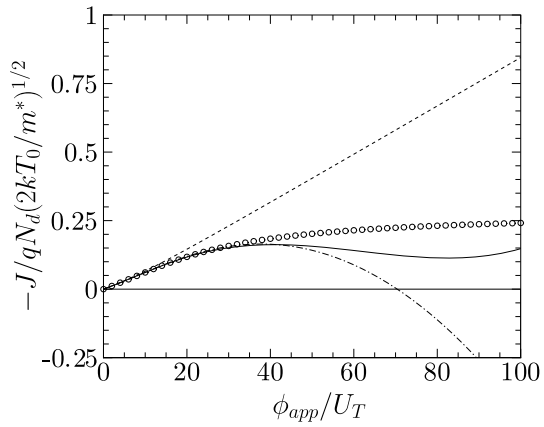
**Fig. 11** Current density  $J$  versus applied potential  $\phi_{app}$  for various Kn with  $\lambda = 0.2$ ,  $N_c/N_d = 0.2$ , and  $D/L = 0.25$ . See the caption of Fig. 7



(a)  $Kn = 0.1$



(b)  $Kn = 0.05$



(c)  $Kn = 0.02$

We recall here that the present asymptotic analysis assumes the magnitude of the applied potential of the order of the thermal potential, i.e.,  $\phi_{app}/U_T = O(1)$ . The present results show that the derived drift-diffusion-type equations are accurate even for larger applied potentials, and thus can be used as a practical tool for computing the current density. On the other hand, we noticed that the curve corresponding to  $\hat{J}^{(2)}$  becomes negative when the applied voltage becomes large. The use of the Yamnahakki's boundary condition, without including the terms up to second order in the Knudsen number, may result in a serious error in practice, when a large applied potential is applied.

Next, we show some results for a different doping profile. In Fig. 9, we show the asymptotic solution of  $(\rho, E, \phi)$  up to order  $\text{Kn}^2$ , together with the corresponding numerical solution of the Boltzmann–Poisson system, for various values of  $\text{Kn}$  with  $(N_c/N_d, D/L) = (0.2, 0.1)$  [the dash-dotted line in Fig. 1(b)] in the case  $\lambda = 1$ . The dependence of these quantities on  $D/L$  is rather weak except for the electric field  $E$ , whose profile clearly depends strongly on the position of the junctions given by  $D/L$ . The asymptotic solutions  $u$  (up to order  $\text{Kn}^3$ ) and  $T$  (up to order  $\text{Kn}^2$ ) as well as the Boltzmann–Poisson solutions, computed with the parameters used in Fig. 9 are similar to those presented in Fig. 5. We also made a numerical comparison for  $(N_c/N_d, D/L) = (0.1, 0.25)$  [the dashed line in Fig. 1(b)]. The result is also similar to that shown in Fig. 5.

Finally, we show some results when  $\lambda$  is relatively small. Figure 10 shows the asymptotic solution of  $(\rho, E, \phi, u, T)$  (up to order  $\text{Kn}^2$  for  $\rho, E, \phi$ , and  $T$ , and up to order  $\text{Kn}^3$  for  $u$ ), as well as the Boltzmann–Poisson solutions, for various values of  $\text{Kn}$  for  $\lambda = 0.2$ . In Fig. 11, the corresponding current-voltage characteristics are displayed. We recall that the asymptotic analysis carried out in Sect. 3 assumes that the scaled Debye length is of order one. Therefore, the present asymptotic expansion is theoretically not applicable to the case of small  $\lambda$ . In spite of this fact, the asymptotic solutions presented in Figs. 10 and 11 exhibit good agreements with the corresponding numerical solutions of the Boltzmann–Poisson system, when  $\phi_{app}/U_T$  is not very large.

## 5 Conclusion

In this paper, we have considered the flow of electrons induced in a semiconductor between two parallel plane contacts. The distribution of the electrons is given by the semiconductor Boltzmann equation with a relaxation-time collision operator of BGK-type. Applying a Hilbert expansion method and Knudsen-layer corrections to the Boltzmann equation, we have derived a drift-diffusion system with higher-order boundary conditions improving results of [11]. The numerical results show a good agreement between the solution of the drift-diffusion model up to order  $\text{Kn}^2$  and that of the Boltzmann–Poisson system if the Knudsen number is not too large and if the Debye length is of the same order as the device length.

The derived drift-diffusion-type equations can be practically used for simulating electron flows in the lightly doped channel region of  $n^+nn^+$  diode. For example, let us choose GaAs at 300 K (permittivity  $\epsilon_s = 13.1\epsilon_0$ ; effective mass  $m^* = 0.0067m_e$ ) with the doping concentration given by  $10^{-13} \text{ cm}^{-3}$ , as in [19]. A typical value for the mobility is  $\mu = 7500 \text{ cm}^2/\text{Vs}$ . This gives the mean free path  $\ell_0 = 0.12 \text{ }\mu\text{m}$  and the Debye length  $\lambda_0 = 1.2 \text{ }\mu\text{m}$ . Therefore, if the channel length is  $L = 1.2 \text{ }\mu\text{m}$ , the corresponding Knudsen number and the scaled Debye length are respectively given by  $\text{Kn} = 0.1$  and  $\lambda = 1$ .

This is the first step of deriving higher-order boundary conditions for fluid-dynamic equations for semiconductors. We expect that our results can be improved by considering more moments in the Boltzmann equation—leading to energy-transport or hydrodynamic models—a more general geometry, improved kinetic inflow boundary con-

ditions [12, 13], or other asymptotic regimes of the semiconductor Boltzmann equation, like the Child-Langmuir regime [39] and the high-field drift-diffusion approximation [40, 41], for instance.

**Acknowledgements** The main part of this work was carried out while S.T. was visiting the Johannes Gutenberg-Universität Mainz as a DAAD (German Academic Exchange Service) fellow. A.J. acknowledges partial support from the Deutsche Forschungsgemeinschaft, grant JU 359/7, and from the Wissenschaftskolleg “Differential Equations” funded by the Fonds zur Förderung der wissenschaftlichen Forschung. This research is part of the ESF program “Global and geometrical aspects of nonlinear partial differential equations (GLOBAL)”.

**Appendix 1: Mean Flow Velocity and Electron Temperature of the Hilbert Solution**

We summarize the Hilbert part of the mean flow velocity,

$$\hat{u}_{H0} = 0, \tag{66}$$

$$\hat{u}_{H1} = -\frac{1}{2} \hat{\tau} \left( \frac{d \ln \hat{\rho}_{H0}}{dx_1} + \hat{E}_{H0} \right), \tag{67}$$

$$\hat{u}_{H2} = -\frac{1}{2} \hat{\tau} \left( \frac{\hat{\rho}_{H1}}{\hat{\rho}_{H0}} \frac{d \ln(\hat{\rho}_{H1}/\hat{\rho}_{H0})}{dx_1} + \hat{E}_{H1} \right), \tag{68}$$

$$\hat{u}_{H3} = -\frac{1}{2} \hat{\tau} \left[ \frac{\hat{\rho}_{H2}}{\hat{\rho}_{H0}} \frac{d \ln(\hat{\rho}_{H2}/\hat{\rho}_{H0})}{dx_1} - \left( \frac{\hat{\rho}_{H1}}{\hat{\rho}_{H0}} \right)^2 \frac{d \ln(\hat{\rho}_{H1}/\hat{\rho}_{H0})}{dx_1} + \hat{E}_{H2} - 2\hat{u}_{H1} \frac{d}{dx_1} (\hat{\tau} \hat{E}_{H0}) \right], \tag{69}$$

and of the electron temperature,

$$\hat{T}_{H0} = 1, \quad \hat{T}_{H1} = 0, \quad \hat{T}_{H2} = -\frac{2}{3} \hat{\tau} \hat{E}_{H0} \hat{u}_{H1} - \frac{2}{3} \hat{u}_{H1}^2, \tag{70}$$

$$\hat{T}_{H3} = -\frac{2}{3} \hat{\tau} (\hat{E}_{H0} \hat{u}_{H2} + \hat{E}_{H1} \hat{u}_{H1}) - \frac{4}{3} \hat{u}_{H1} \hat{u}_{H2}. \tag{71}$$

**Appendix 2: Comments on the Numerical Solution of the Knudsen-layer Problems**

Let us introduce the functions  $g_m(\eta', \zeta_y, \zeta_2, \zeta_3)$  ( $m = 1, 2, 3, 4$ ) which are the solutions of the following half-space boundary-value problems:

$$\zeta_y \frac{\partial g_m}{\partial \eta'} = \Omega_m - g_m + I h_m, \tag{72}$$

$$\Omega_m(\eta') = \int g_m \mathcal{M} d^3 \bar{\zeta}, \tag{73}$$

$$g_m = -a_m + \mathcal{J}_m \quad (\text{for } \zeta_y > 0, \text{ at } \eta' = 0), \tag{74}$$

$$g_m \rightarrow 0 \quad (\text{as } \eta' \rightarrow \infty), \tag{75}$$

with

$$I h_1 = I h_2 = 0, \quad I h_3 = \frac{1}{2} \frac{\partial g_1}{\partial \zeta_y} - \zeta_y g_1, \quad I h_4 = -\eta' (\Omega_1 - \psi_1)$$

and  $\mathcal{J}_1 = -2\zeta_y$ ,  $\mathcal{J}_2 = 2\zeta_y^2$ , and  $\mathcal{J}_3 = \mathcal{J}_4 = 0$ . Here,  $a_m$  are constants to be determined together with the solutions. Then  $(\xi_1, \psi_1)$ ,  $(\xi_{2a}, \psi_{2a})$ ,  $(\xi_{2b}, \psi_{2b})$ , and  $(\xi_{2c}, \psi_{2c})$  introduced in the main text [(55) and (56)] are given by

$$\begin{aligned}(\xi_1, \psi_1) &= (\xi_{2a}, \psi_{2a}) = (a_1, g_1), & (\xi_{2b}, \psi_{2b}) &= (a_2 + a_3 - 1, g_2 + g_3), \\ (\xi_{2c}, \psi_{2c}) &= (a_4, g_4).\end{aligned}$$

Our aim is to obtain the slip coefficients  $a_m$  and the Knudsen-layer functions  $\Omega_m(\eta')$  numerically. In this appendix, we give a brief comment on the numerical method.

By taking advantage of the simple expression of the relaxation-time collision operator, we can transform the equation and boundary conditions (72–75) to an integral equation for  $\Omega_m(\eta')$ . This is done by integrating (72) formally under the boundary conditions (74) and (75), inserting the result into (73), and carrying out the integration with respect to the velocity space. The resulting equation contains only  $\eta'$  as an independent variable, and thus the problem simplifies significantly. Moreover, we can avoid the singularity contained in  $Ih_3$  of the original form [note that  $g_1$  or, in general,  $g_m$  has a discontinuity at  $\eta' = 0$  with respect to  $\zeta_y$ , i.e.  $\lim_{\zeta_y \rightarrow 0^+} g_1(0, \zeta_y, \zeta_2, \zeta_3) \neq \lim_{\zeta_y \rightarrow 0^-} g_1(0, \zeta_y, \zeta_2, \zeta_3)$ ].

The integral equations for  $\Omega_1$  and  $\Omega_2$  are identical with those for the Knudsen-layer problems of rarefied gas flows around a boundary, derived from the linearized BGK model of the Boltzmann equation. More precisely, the equations for  $\Omega_1$  and  $\Omega_2$  are respectively identical with the equation for the Knudsen layer in shear flow over a flat wall [42–45] and in thermal-creep flow over a flat wall [46]. The numerical solutions to these equations are obtained in [25, 26, 43–45] (also see [24, 31, 47]). Concerning the equation for  $\Omega_3$ , the same type of integral equation has been solved numerically in [48]. Therefore, we can make use of the numerical data given in these references. For example,  $[a_1, \Omega_1(x)] = [2k_0, 2Y_0(x)]$  in [24, 31, 47],  $[a_2, \Omega_2(x)] = [1 - 4K_1, -2Y_1(x)]$  in [31, 47], and  $[a_3, \Omega_3(x)] = [a_2 + 2k_0^2 + 8K_1, -2\tilde{Y}_0(x) + 2k_0Y_0(x) + 4Y_1(x)]$  in [31]. In the cited works, the integral equations are solved by means of a moment method devised by Sone [43, 49] and improved by Sone and Onishi [47, 50]. We employ this method in order to obtain the numerical solution  $\Omega_4(\eta')$  and  $a_4$  in the present study.

## References

1. Van Roosbroeck, W.: Theory of flow of electrons and holes in germanium and other semiconductors. *Bell Syst. Tech. J.* **29**, 560 (1950)
2. Bløtebjerg, K.: Transport equations for electrons in two-valley semiconductors. *IEEE Trans. Electron. Devices* **17**, 38 (1970)
3. Stratton, R.: Diffusion of hot and cold electrons in semiconductor barriers. *Phys. Rev.* **126**, 2002 (1962)
4. Ben Abdallah, N., Degond, P.: On a hierarchy of macroscopic models for semiconductors. *J. Math. Phys.* **37**, 3306 (1996)
5. Ben Abdallah, N., Degond, P., Génieys, S.: An energy-transport model for semiconductors derived from the Boltzmann equation. *J. Stat. Phys.* **84**, 205 (1996)
6. Degond, P., Génieys, S., Jüngel, A.: A system of parabolic equations in nonequilibrium thermodynamics including thermal and electrical effects. *J. Math. Pures Appl.* **76**, 991 (1997)
7. Ben Abdallah, N., Desvillettes, L., Génieys, S.: On the convergence of the Boltzmann equation for semiconductors toward the energy transport model. *J. Stat. Phys.* **98**, 835 (2000)
8. Degond, P., Jüngel, A., Pietra, P.: Numerical discretization of energy-transport models for semiconductors with non-parabolic band structure. *SIAM J. Sci. Comput.* **22**, 986 (2000)
9. Anile, A., Muscato, O.: Improved hydrodynamic model for carrier transport in semiconductors. *Phys. Rev. B* **51**, 16728 (1995)
10. Grasser, T., Kosina, H., Gritsch, M.: Using six moments of Boltzmann's transport equation for device simulation. *J. Appl. Phys.* **90**, 2389 (2001)

11. Yamnahakki, A.: Second order boundary conditions for the drift-diffusion equations for semiconductors. *Math. Models Methods Appl. Sci.* **5**, 429 (1995)
12. Cercignani, C., Gamba, I.M., Levermore, C.D.: A drift-collision balance for a Boltzmann–Poisson system in bounded domains. *SIAM J. Appl. Math.* **61**, 1932 (2001)
13. Ringhofer, C., Schmeiser, C., Zwirchmayr, A.: Moment methods for the semiconductor Boltzmann equation on bounded position domains. *SIAM J. Numer. Anal.* **39**, 1078 (2001)
14. Baranger, H.U., Wilkins, J.W.: Ballistic structure in the electron distribution function of small semiconducting structures: General features and specific trends. *Phys. Rev. B* **36**, 1487 (1987)
15. Baranger, H.U., Wilkins, J.W.: *Phys. Rev. B* **30**, 7349 (1984)
16. Trugman, S.A., Taylor, A.J.: Analytic solution of the Boltzmann equation with applications to electrons transport in inhomogeneous semiconductors. *Phys. Rev. B* **33**, 5575 (1986)
17. Kuhn, T., Mahler, G.: Carrier kinetics in a surface-excited semiconductor slab: Influence of boundary conditions. *Phys. Rev. B* **35**, 2827 (1987)
18. Sano, N.: Kinetic study of velocity distributions in nanoscale semiconductor devices under room-temperature operation. *Appl. Phys. Lett.* **85**, 4208 (2004)
19. Csontos, D., Ulloa, S.E.: Quasiballistic, nonequilibrium electron distribution in inhomogeneous semiconductor structures. *Appl. Phys. Lett.* **86**, 253103 (2005)
20. Poupaud, F.: Diffusion approximation of the linear semiconductor Boltzmann equation: Analysis of boundary layers. *Asymptot. Anal.* **4**, 293 (1991)
21. Golse, F., Poupaud, F.: Limite fluide des équations de Boltzmann des semi-conducteurs pour une statistique de Fermi–Dirac. *Asymptot. Anal.* **6**, 135 (1992)
22. Bardos, C., Santos, R., Senti, R.: Diffusion approximation and computation of the critical size. *Trans. Am. Math. Soc.* **284**, 617 (1984)
23. Degond, P., Schmeiser, C.: Kinetic boundary layers and fluid-kinetic coupling in semiconductors. *Trans. Theory Stat. Phys.* **28**, 31 (1999)
24. Sone, Y.: Asymptotic theory of flow of rarefied gas over a smooth boundary I. In: Trilling, L., Wachman, H.Y. (eds.) *Rarefied Gas Dynamics*, vol. 1, p. 243. Academic Press, New York (1969)
25. Sone, Y., Yamamoto, K.: Flow of rarefied gas over plane wall. *J. Phys. Soc. Jpn.* **29**, 495 (1970)
26. Sone, Y., Onishi, Y.: *J. Phys. Soc. Jpn.* **47**, 672 (1979)
27. Sone, Y.: Asymptotic theory of flow of rarefied gas over a smooth boundary II. In: Dini, D. (ed.) *Rarefied Gas Dynamics*, vol. 2, p. 737. Editrice Tecnico Scientifica, Pisa (1971)
28. Sone, Y.: Asymptotic theory of a steady flow of a rarefied gas past bodies for small Knudsen numbers. In: Gagnol, R., Soubbaramayer. (eds.) *Advances in Kinetic Theory and Continuum Mechanics*, p. 19. Springer, Berlin (1991)
29. Sone, Y., Aoki, K., Takata, S., Sugimoto, H., Bobylev, A.V.: Inappropriateness of the heat-conduction equation for description of a temperature field of a stationary gas in the continuum limit: Examination by asymptotic analysis and numerical computation of the Boltzmann equation. *Phys. Fluids* **8**, 628 (1996). Erratum **8**, 841 (1996)
30. Sone, Y., Bardos, C., Golse, F., Sugimoto, H.: Asymptotic theory of the Boltzmann system, for a steady flow of a slightly rarefied gas with a finite Mach number: General theory. *Eur. J. Mech. B/Fluids* **19**, 325 (2000)
31. Sone, Y.: *Kinetic Theory and Fluid Dynamics*. Birkhäuser, Boston (2002)
32. Sone, Y.: *Molecular Gas Dynamics: Theory, Techniques, and Applications*. Birkhäuser, Boston (2006)
33. Aoki, K., Takata, S., Nakanishi, T.: Poiseuille-type flow of a rarefied gas between two parallel plates driven by a uniform external force. *Phys. Rev. E* **65**, 026315 (2002)
34. Bhatnagar, P.L., Gross, E.P., Krook, M.: A model for collision processes in gases I. Small amplitude processes in charged and neutral one-component systems. *Phys. Rev.* **94**, 511 (1954)
35. Welander, P.: On the temperature jump in a rarefied gas. *Ark. Fys.* **7**, 507 (1954)
36. Kogan, M.N.: On the equations of motion of a rarefied gas. *Appl. Math. Mech.* **22**, 597 (1958)
37. Chu, C.K.: Kinetic-theoretic description of the formation of a shock wave. *Phys. Fluids* **8**, 12 (1965)
38. Aoki, K., Nishino, K., Sone, Y., Sugimoto, H.: Numerical analysis of steady flows of a gas condensing on or evaporating from its plane condensed phase on the basis of kinetic theory: Effect of gas motion along the condensed phase. *Phys. Fluids A* **3**, 2260 (1991)
39. Ben Abdallah, N., Degond, P.: The Child–Langmuir law for the Boltzmann equation of semiconductors. *SIAM J. Math. Anal.* **26**, 364 (1995)
40. Poupaud, F.: Runaway phenomena and fluid approximation under high fields in semiconductor kinetic theory. *Z. Angew. Math. Mech.* **72**, 359 (1992)
41. Cercignani, C., Gamba, I., Levermore, C.: High field approximations to a Boltzmann–Poisson system and boundary conditions in a semiconductor. *Appl. Math. Lett.* **10**, 111 (1997)
42. Willis, D.R.: Comparison of kinetic theory analyses of linearized Couette flow. *Phys. Fluids* **5**, 127 (1962)

43. Sone, Y.: Kinetic theory analysis of linearized Rayleigh problem. *J. Phys. Soc. Jpn.* **19**, 1463 (1964)
44. Sone, Y.: Some remarks on Knudsen layer. *J. Phys. Soc. Jpn.* **21**, 1620 (1966)
45. Tamada, K., Sone, Y.: Some studies on rarefied gas flows. *J. Phys. Soc. Jpn.* **21**, 1439 (1966)
46. Sone, Y.: Thermal creep in rarefied gas. *J. Phys. Soc. Jpn.* **21**, 1836 (1966)
47. Sone, Y., Onishi, Y.: Kinetic theory of evaporation and condensation—hydrodynamic equation and slip boundary condition. *J. Phys. Soc. Jpn.* **44**, 1981 (1978)
48. Sone, Y., Yamamoto, K.: Flow of rarefied gas through a circular pipe. *Phys. Fluids* **11**, 1672 (1968). Erratum **13**, 1651 (1970)
49. Sone, Y.: Effect of sudden change of wall temperature in rarefied gas. *J. Phys. Soc. Jpn.* **20**, 222 (1965)
50. Sone, Y., Onishi, Y.: Kinetic theory of evaporation and condensation. *J. Phys. Soc. Jpn.* **35**, 1773 (1973)